REPORT No. 53

REPORT No. 53

X

THE COLLEGE OF AERONAUTICS
CRANFIELD

AN INVESTIGATION OF THE NOISE FIELD FROM A SMALL JET AND METHODS FOR ITS REDUCTION

by

R. WESTLEY, B.Sc., D.C.Ae.
and
G. M. LILLEY, M.Sc., D.I.C., A.F.R.Ae.S.
of the Department of Aerodynamics.

Price 5s.

COLLEGE REPORT NO. 53

ERRATA SHEET

Page 7 ... Line 4 ... Delete 'phons'. Insert 'decibels'.

Line 5 ... Delete 'decibels'. Insert 'phons'.

Line 6 ... Insert 'above' before the number '6000'.

Line 14 ... Delete 'therefore'.

Line 16 and 17 ... Delete the words 'although the measured values are in P phons'.

Line 33 ... Equation 3.5 should read

$$M_1^2 = \frac{2}{\gamma-1}\left[(1+\mathcal{P})^{\frac{\gamma-1}{\gamma}} - 1\right]$$

Page 9 ... Line 7 ... Delete 'phons'. Insert 'decibels'.

Page 15 .. Line 14 ... Delete 'significant'. Insert 'suggested'.

Figure 32 ... Delete '$\mathcal{P} = 0.9$'. Insert '$\mathcal{P} = 1.33$'.

Report No. 53

January 1952.

THE COLLEGE OF AERONAUTICS

CRANFIELD

An Investigation of the Noise Field from a Small Jet and Methods for its Reduction

- by -

R. Westley, B.Sc., D.C.Ae.*

and

G.M. Lilley, M.Sc., D.I.C., A.F.R.Ae.S.

of the Department of Aerodynamics.

--ooOoo--

SUMMARY

Sound measurements have been made on the noise from the jet of a one inch diameter convergent nozzle at atmospheric temperature and at speeds above and below choking. The noise level and spectrum have been investigated in both the near and distant fields. The results agree in some measure with the predictions of the Lighthill theory, that the elementary sound radiator is an acoustic quadrupole. The agreement is more marked if attention is confined to the higher frequencies.

Simple empirical formulae are derived giving the overall sound intensity and frequency spectrum in terms of the position relative to the jet, the stagnation pressure excess over the atmospheric pressure, and the frequency.

The results of tests on various noise reduction devices are discussed. These tests indicate promising lines of investigation. The maximum reduction in total noise level was about 10 db.

- - - - - -

YSB

---

* This author was the holder of a Busk Studentship throughout this investigation.

C O N T E N T S

CONTENTS (contd.)

Figures (contd.)

CONTENTS (contd.)

Figures (contd.)

1. NOTATION

a	speed of sound.
A	nozzle area.
d	nozzle exit diameter.
D	throat of diffuser } see noise
h	gap between diffuser and nozzle } reduction devices.
H	total head in jet.
I	sound intensity.
I_{th}	sound intensity at the threshold of hearing (10^{-16} watts per sq. cm.).
I_n	spectral density.
M	Mach number.
n	frequency.
N	sound level in decibels.
P	loudness in phons.
$\sqrt{\overline{p^2}}$	root mean square value of pressure fluctuations.
p	static pressure.
T	temperature.
t	time.
x,r	cylindrical coordinates of the microphone with the nozzle exit as origin and the jet axis as abscissa.
$\tilde{\omega},\theta$	spherical polar coordinates of the microphone with the nozzle exit as origin and the jet axis as the datum.
U	velocity in direction of jet axis.
γ	ratio of specific heats and the angle of nozzle teeth.
δ	diffuser angle.
λ	wave length.
μ	coefficient of viscosity.
ν	kinematic viscosity.
ρ	density.
τ	shear stress.
$\mathcal{P}=\frac{p_s-p_o}{p_o}$	nozzle pressure ratio.

Suffix s denotes conditions at the contraction entry.
o denotes conditions in the atmosphere.
1 denotes conditions at the nozzle exit.

2. INTRODUCTION

In this report the following definitions of boundary layer, jet and aerodynamic noise are used.

DEFINITIONS

Boundary layer noise is the noise created in the boundary layer of moving fluids adjacent to solid surfaces (due either to the turbulence or some other cause).

Jet noise is the noise created in the mixing region between a jet of moving fluid and an external medium due to the presence of turbulence or some other vortex motion. This excludes mechanical noise, in particular noise due to rotating machinery.

Aerodynamic noise is noise resulting from air in motion and includes both boundary layer and jet noise. It also covers such noise as that arising from the wakes of bluff obstacles and that created inside ducts.

It is well known that air jets and boundary layers cause noise. At present, however, very little is understood about how the noise is caused. Interest in this subject has recently increased with the high speeds and jet engines of modern aircraft. Noise is now a serious and growing source of distress to passengers in aircraft and to persons on the ground.

An allied problem which initially prompted the investigation of aerodynamic noise arose in the interpretation of measurements made in a low turbulence wind tunnel. In a low turbulence wind tunnel it is difficult to differentiate between fluctuations in velocity due to noise and turbulence. It was considered that measurements both of noise and turbulence in an air jet would be a convenient means of making a preliminary attack on this problem.

The present series of experiments were planned

(a) to make measurements of noise level and frequency around an air jet at speeds above and below choking so as to provide data enabling the problem of noise creation in the jet to be studied,

(b) to check existing theories, notably the Lighthill theory, on jet noise,

(c) to investigate devices for jet noise reduction.

The principal theoretical contribution to the noise created in boundary layers and jet is that due to Lighthill[1]. The papers by Billing[2] on moving sources of sound, the estimation of pressure fluctuations in isotropic turbulence by Batchelor[3] and on stellar dipoles and quadrupoles by Schwarzschild[4] represent the only additional theoretical work on this subject. A recent paper by Powell[5] has reported some interesting experimental work in connection with the visualisation of sound waves from a converging jet at speeds above choking.

where

A_1 = area of nozzle exit (sq. ft.)

p_o = atmospheric pressure (lb. per sq.ft.)

T_s = temperature at contraction entry (^oK).

U_1 = speed at nozzle exit (f.p.s.).

Reynolds Number

The Reynolds number, based on the nozzle exit diameter and the jet exit speed, of the tests described in this report, can be obtained from the relation

$$\frac{R}{M_1} = 0.59 \times 10^6 \qquad \ldots\ldots (3.8)$$

where

$$R \equiv \frac{\rho_1 U_1 d}{\mu_1}$$

M_1 = Mach number at the nozzle exit.

4. APPARATUS

Test rig.

The noise measurements were made with a horizontal air jet which emerged from a circular nozzle of one inch diameter. The nozzle was placed fifteen feet above ground level and about fifteen feet from the nearest building in order to reduce sound reflections. A side view of the test rig is shown in Figure 1 and a plan view of the jet site in Figure 2. Additional views of the rig are shown in Figures 3 and 4.

The air compressor, cooler and settling tank were situated in the main laboratory and were connected to the jet by about 30 feet of 6 inch diameter iron piping. The piping passed through two brick walls to the outside of the laboratory, through a gate control valve and then up over a supporting pylon to a contraction and the nozzle. The contraction had an area ratio of 36:1 and was designed by the method given in Reference 6 to give a monotonic increase in velocity along the boundary wall from entry to exit. A gauze screen was fitted at the contraction entry.

During each test the compressor was run continuously. Except at very low jet speeds, the noise from the compressor reaching the microphone placed in the jet field was small compared with the jet noise. The jet speed was maintained steady by adjusting the compressor inlet valve and the gate control valve. The pressure drop across the latter was kept as small as possible in order to avoid further noise. The air supplied to the jet was undried but condensed water vapour was drained off from the settling tank and the vertical pipe leading to the nozzle. No icing up of the jet nozzle occurred.

The static pressure at the contraction entry was measured on a mercury manometer.

Noise measuring apparatus

The jet noise was measured using a 74100-C objective noise meter together with a 74101-A octave filter, both manufactured by Standard Telephones Ltd. As already noted, this apparatus records noise levels in phons (50-140) above a threshold intensity of 10^{-16} watts per sq. cm. The octave filter has 16 ranges and noise levels in any of the following frequency bands may be measured.

Octave Number	Frequency Band (cycles per second)	Octave Number	Frequency Band (cycles per second)
11	37.5 - 75	21	50 - 100
12	75 - 150	22	100 - 200
13	150 - 300	23	200 - 400
14	300 - 600	24	400 - 800
15	600 -1200	25	800 - 1600
16	1200 -2400	26	1600 - 3200
17	2400 -4800	27	3200 - 6400
18	4800 -9600	28	6400 -12800

The microphone, of the moving coil type, was sensitive over the range 50 - 10,000 c/s. The sensitivity was not constant over the whole frequency range and a 'microphone correction' had to be applied as follows.

Octave Number	Correction	Octave Number	Correction
28	Add + 5.5 db.	24	+ 1.0
18	+ 6.0	14	+ 1.0
27	+ 5.0	23	+ 0.5
17	+ 5.5	13	+ 0.0
26	+ 4.5		
16	+ 4.0		
25	+ 3.0		
15	+ 2.5		

An additional correction was necessary to the lower octave readings if high noise levels were present in the higher octaves. For this reason it has been necessary to discount a large number of readings obtained in the octaves below 13. The contribution to the total noise, from these lower frequencies, was however very small.

Distant noise field tests were made with the microphone pointing towards the jet nozzle. The microphone was set in the horizontal plane containing the jet axis. It was loosely suspended by rubber strips in a wire box frame 15 in. x 15 in. x 15 in. The frame was covered with muslin to prevent atmospheric winds blowing on the microphone. The frame was supported by a vertical pole 15 ft. high. The position of the microphone was located with the aid of a theodolite.

Near noise field tests were made with the microphone in a vertical plane below the jet axis and pointing towards the axis. The microphone was supported on a moveable beam and no wind shield was fitted.

Total head traverses were made across the jet at various stations downstream of the jet exit. The pitot tube was made of hyperdermic tubing of 1.0 mm. external diameter. The pressures were measured on a mercury manometer.

Noise reduction devices

The nozzle end of the contraction was constructed so as to permit the connection of various noise reducing devices (see Figures 5 and 6). These devices were as follows:-

(a) A cylindrical wire gauze extension of 1 inch diameter and 1.5 inches long (see Figure 7b). The mesh of the gauze was 30 per inch.

(b) A slotted extension (see Figure 5b).

This was 1.75 inches long and the slots, at 0.75 inches from the end, were alternatively bent inwards and outwards.

(c) Teeth extension (see Figures 5c, 1, 2, 3, 4).

The teeth were set at various angles γ^{o} (positive if inwards) to the jet axis.

c.1.	Six teeth	0.25 in x 0.25 in.
c.2.	Twelve teeth	0.125 in x 0.125 in.
c.3.	Twenty-four teeth	0.0625 in x 0.0625 in.
c.4.	Six teeth	0.125 in x 0.375 in.
	Six teeth	0.125 in x 0.25 in.

(d) Diffuser and slot (see Figure 5)

A circumferential slot of variable width was situated at the throat of the diffuser.

5. SCOPE OF TESTS

The tests may be grouped under the following headings:

A. The distant sound field.

B. The near sound field.

C. The velocity distribution in the jet.

D. Noise reduction devices.

A. The distant sound field

The variation of noise level with $\tilde{\omega}$ (θ = constant)

Test 1	Total Noise	$\mathcal{P}$	= 0.67	$\theta = 30^{\circ}$
2	" "	$\mathcal{P}$	= 0.9	$\theta = 30^{\circ}$
3	" "	$\mathcal{P}$	= 1.17	$\theta = 30^{\circ}$
4	" "	$\mathcal{P}$	= 1.5	$\theta = 30^{\circ}$
5	Octave Noise	$\mathcal{P}$	= 1.0	$\theta = 45^{\circ}$.

The variation of noise level with θ ($\tilde{\omega}$ = constant)

The noise level was recorded for various values of $\mathcal{P}$ at a radius of $\tilde{\omega}/d = 108$.

Test 6	Total Noise	$\mathcal{P}$	= 0.9	$\tilde{\omega}/d = 108$
7	" "	$\mathcal{P}$	= 1.2	$\tilde{\omega}/d = 108$
8	Octave "	$\mathcal{P}$	= 0.9	$\tilde{\omega}/d = 108$.

The variation of noise level with $\mathcal{P}$ ($\tilde{\omega}$ = constant)

The noise level was recorded for various values of $\mathcal{P}$ from 0 to 2.0 at a constant value of $\tilde{\omega}/d = 108$.

Test 9	Total and Octave Noise	$\theta = 30^{\circ}$	$\tilde{\omega}/d = 108$
10	" " " "	$\theta = 45^{\circ}$	$\tilde{\omega}/d = 108$
11	" " " "	$\theta = 60^{\circ}$	$\tilde{\omega}/d = 108$
12	" " " "	$\theta = 75^{\circ}$	$\tilde{\omega}/d = 108$
13	" " " "	$\theta = 90^{\circ}$	$\tilde{\omega}/d = 108$.

B. The near sound field

Test 14	Total and Octave Noise	$\mathcal{P}$	= 0.9	r,x variable
15	" " " "	$\mathcal{P}$	= 1.33	r,x variable.

C. The velocity distribution in the jet

Total head traverses were made at several stations along the jet axis.

Test 16 $\frac{H - p_o}{p_o}$ at $\frac{x}{d}$ = 0.5, 1, 3, 6, 9, 12, 15, 18, 24.

D. The noise reduction devices

These devices were tested at various speeds with the microphone at $\bar{\omega}/d$ = 108 and $\theta = 30^\circ$. The effect of variations in the teeth angle γ° was noted.

Test 17	Total and octave noise					Wire gauze extension
18	"	"	"	"		Slotted extension
19	"	"	"	"	c.1	3 at $\gamma = 0^\circ$: 3 at $\gamma = 0^\circ$
20	"	"	"	"	c.1	3 at $\gamma = 30^\circ$: 3 at $\gamma = -30^\circ$
21	"	"	"	"	c.1	3 at $\gamma = 30^\circ$: 3 at $\gamma = 0^\circ$
22	"	"	"	"	c.1	3 at $\gamma = 15^\circ$: 3 at $\gamma = 0^\circ$
23	"	"	"	"	c.1	3 at $\gamma = 15^\circ$: 3 at $\gamma = -15^\circ$
24	"	"	"	"	c.1.	3 at $\gamma = 45^\circ$: 3 at $\gamma = -45^\circ$
25	"	"	"	"	c.1	3 at $\gamma = 45^\circ$: 3 at $\gamma = 0^\circ$
26	"	"	"	"	c.1	3 at $\gamma = 30^\circ$: 3 at $\gamma = 30^\circ$
27	"	"	"	"	c.2	6 at $\gamma = 30^\circ$: 6 at $\gamma = 0^\circ$
28	"	"	"	"	c.3.	12 at $\gamma = 90^\circ$: 12 at $\gamma = 90^\circ$
29	"	"	"	"	c.3.	12 at $\gamma = 30^\circ$: 12 at $\gamma = 0^\circ$
30	"	"	"	"	c.4	6 - 0.125 x 0.25 x $\gamma = 0^\circ$
						6 - 0.125 x 0.375 x $\gamma = +30^\circ$
31	Total noise					Diffuser and slot.

Visual observation by means of a standard schlieren and shadowgraph installation was made of the jet with and without the noise reduction devices.

6. DETAILS OF RESULTS

The atmospheric pressure p_o, atmospheric temperature T_o, and the jet stagnation temperature T_s were recorded during each test. These quantities varied according to the daily atmospheric conditions. The noise level meter was not of sufficient accuracy to detect any changes of noise intensity due to these

variations. Mean values of p_o, T_o and T_s were

$$p_o = 29.9 \pm 0.5 \text{ in. Hg.}$$
$$T_o = 10^o \pm 10^o \text{ C.}$$
$$T_s = 17^o \pm 5^o \text{ C.}$$

The curves of noise level at each octave are labelled in each diagram where possible with the appropriate octave number. In order to distinguish the curves at various parts of the speed range, where intersection occurs, the following set of symbols will be used:

Octave Number	28	18	27	17	26	16
Frequency	12,800	9,600	6,400	4,800	3,200	2,400
	-6,400	-4,800	-3,200	-2,400	-1600	-1,200
Symbol	⊙	•	×	↖	△	⩒

Octave Number	25	15	24	14	23	13	22	12
Frequency	1600	1200	800	600	400	300	200	150
	- 800	-600	-400	-300	-200	-150	-100	- 75
Symbol	∼	,	⊡	✱	◥	▽	+	Y

Octave Number	21	11	Total Noise
Frequency	100	75	
	- 50	-37.5	
Symbol	◠	◈	❁

A. <u>The distant noise field</u>

<u>The variation of noise level with $\tilde{\omega}$</u>

The noise level is plotted against $\log(\tilde{\omega}/d)$ in Figure 7. The results show that for $\tilde{\omega}/d > 50$ the noise intensity follows an inverse square law

$$I \sim 1/\tilde{\omega}^2$$

for both high and low frequencies and for total noise. The result is true for speeds above and below choking.

<u>The variation of total noise level with θ</u>

The total noise level is plotted against θ, in Figure 8, for values of θ up to 150^o. It was found impossible to take accurate measurements at less than 20^o. These results show that a maximum occurs at $\theta = 28^o$ and the noise level then decreases as the jet is approached.

The variation of octave noise level with θ

The octave noise level is plotted against θ in Figure 9. The results show a similar trend to those in Figure 8, but the values of θ for maximum noise intensity, θ_{max}, vary in each frequency band as follows:

Frequency c/s	300 -600	400 -800	600 -1200	800 -1600	1200 -2400	1600 -3200	2400 -4800	3200 -6400	4800 -9600	6400 -12800
$\theta_{max.}$	$<20^\circ$	$<20^\circ$	$<20^\circ$	20°	25°	25°	26°	31°	38°	45°

It is significant that the angle of maximum noise increases as the frequency increases. (A lower maximum at $\theta = 100^\circ$ occurs at the high frequencies. This is probably due to experimental error but is worth further investigation.)

The variation of octave noise level with frequency (Octave number)

The octave noise level is plotted against octave number (or log n) in Figure 10. It is shown that the noise spectrum is roughly similar at all angles. The octave number for maximum noise at a given value of θ is as follows:

θ	150°	120°	90°	60°	30°	20°
frequency c/s at maximum noise	3200 -6400	3200 -6400	3200 -4800	3200 -4800	2400 -4800	1600 -2400
octave number	27	27	17-27	17-27	17	26-17.

The variation of noise level with $\mathcal{P}$

The noise level is plotted against $\mathcal{P}$ in Figures 11-15 inclusive. In Figure 11 it can be seen that above choking ($\mathcal{P} \geq 0.893$) the results for octaves lower than 14 not only register equal noise levels but have slopes similar to those corresponding to the highest frequencies. It is suggested that the octave filter was leaking from the high frequency to the low frequency bands at the high noise levels. Although the readings in the lower octaves at low total noise levels appeared to be correct the results for all octaves below 14 have been discarded, except for measurements in the near sound field.

It is shown that a maximum occurs at about $\mathcal{P} = 1.1$ followed by a minimum at about $\mathcal{P} = 1.3$. A rapid rise in noise intensity then follows.

Figure 15 shows that for $\theta = 30^\circ$ a second peak occurs at $\mathcal{P} = 1.8$ for the highest frequency. These latter results show very great irregularities above choking.

The background noise, with the jet turned off was as follows:

Octave number	13	23	14	24	15	25	16	26	17	27	18	28
Octave Noise (db)	60	62	60	55	<50	<50	<50	<50	<50	<50	<50	<50

The rate of increase of noise intensity with jet speed

The results from Figure 11 have been replotted in Figure 16 using a logarithm scale for abscissa. Similar results are obtained from Figures 12 to 15 inclusive. It is shown that when $\mathcal{P} < 1$ and > 1.2 the intensity, both total and octave, follows the law

$$I \sim \mathcal{P}^b$$

where the index b is a function both of frequency and θ. The values of b, below choking, are plotted against θ in Figure 17. It is significant that the value of b approaches the value of 4 as θ tends to zero. Between $\theta = 30^\circ$ and $\theta = 90^\circ$ the mean value of b, below choking, is about 2.5 and above choking at the higher frequencies is about 8.5.

From a cross plot of the above results the angle for maximum total noise intensity can be plotted as a function of jet speed. This is shown in Figure 18. The very marked change, with jet speed, in the character of the jet as a sound producer, is apparent. It should be noted that the greatest changes appear to occur below choking. Above choking the angle for maximum noise intensity lies inside the jet boundaries.

The variation of the noise spectrum with jet speed

The effect of jet speed on the noise spectrum is shown in Figures 19-23 inclusive. It can be seen that the spectrum is similar for all speeds in the range $0.3 < \mathcal{P} < 1.3$. The maximum noise intensity shifts slightly towards the higher frequencies as the jet speed is increased.

B. The near noise field

The average of a large number of results has been plotted as sound contour lines (lines of equal sound intensity) in Figures 24-30 inclusive for a value of $\mathcal{P} = 0.9$ and in Figures 31-33 inclusive for a value of $\mathcal{P} = 1.33$. The diagrams are drawn for both total noise contours and octave noise contours. The low frequency contour diagrams (apart from octave 11) have been discounted, for the reasons stated above, and have not been reproduced. The contour line diagrams for octave 11 shown in Figures 30 and 33 show marked differences from the higher frequency diagrams beyond a distance of about 20 diameters from the nozzle exit. Since the high frequency noise level in this region is considerably lower than in the regions near to the nozzle exit, it is considered that the portion of the lowest frequency diagrams beyond, say, 20 diameters may be reliable.

The various contour diagrams clearly show that the jet contains a distribution of sound sources the extent of which increases in the downstream direction as the frequency is decreased. The approximate extent of these sources along the jet axis at $\mathcal{P}$ = 0.9 is as follows:

	Position of noise sources
Total noise	0 - 30 diameters
Octave 28	0 - 10
27	0 - 14
26	0 - 16
25	0 - 18
24	0 - 24
11	Commencing at about 25 diameters and extending to distances far downstream.

It can be seen that although the total intensity contour lines do not show marked directional characteristics, the contour lines at high frequencies show maxima at 45° to the jet axis measured from an origin coincident with the downstream position of the source distribution in the appropriate frequency band.

With the origin of coordinates at the nozzle exit, the direction of maximum noise approaches the jet axis as the frequency is reduced. This result confirms the observations made in the distant noise field.

The contour diagrams above do not extend to the regions upstream of the nozzle. Measurements obtained in this region, at various frequencies, did show a second maximum of lower magnitude at the highest frequencies, but the increase in noise level was only about 2 db. and in general the contours showed regular continuations of the lines in the downstream region.

C. The velocity distribution in the jet

The distribution of total head at various stations along the jet axis at $\mathcal{P}$ = 0.9 is shown in Figure 34. Figure 35, which shows the variation of total head along the jet axis, indicates that the central core of the jet extends to about 4.5 diameters downstream of the nozzle exit. The jet boundaries are shown in Figure 36. The outer boundary makes an angle of 6.5° to the jet axis, whilst the corresponding angle of the inner boundary is 5.5°. Figure 36 also shows the lines of constant total head and the line of maximum total head gradient.

The boundary layer thickness at the nozzle exit was 0.08 diameters.

D. Noise reducing devices

Lighthill[1] has shown that the sound intensity is proportional to the square of the velocity gradient. It was considered, therefore, that a reduction in the noise intensity would be obtained by the use of devices which would reduce the rate of shear. Only those devices which did not cause excess blockage were tested.

It was found, at a very early stage in the investigation, that a drop of 10 db. in noise intensity could be obtained if a solid object projected into the jet boundary.

(a) The wire gauze extension

Below $\mathcal{P} = 1$ no change in noise level was obtained. Above this value of excess pressure ratio a reduction of 5 db. occurred. The effect of the gauze was to delay the rapid noise increase which was present above $\mathcal{P} = 1$ (this increase can be seen in Figure 11). An optical investigation, see Figures 37a and 37b, showed that the train of shock waves, present above choking, were eliminated by the introduction of the gauze. In the latter case, an outflow took place through the gauze, the flow expanded inside the gauze, and the jet emerged as a supersonic stream free from expansion and shock waves. As the pressure increased still further the length of gauze was insufficient to allow a complete expansion down to atmospheric pressure. The shock pattern then began to reform with a corresponding rapid increase in noise level.

(b) and (c) The effect of teeth extensions to the nozzle

The noise levels for thirteen different teeth configurations are compared with the unmodified nozzle results in Figure 38. The corresponding noise spectrum variations are shown, for $\mathcal{P} = 0.67$ and $\mathcal{P} = 2.0$, in Figures 39 and 40 respectively. It will be seen that reductions in noise level of 5 db. below choking and 12 db. above choking can be obtained with six teeth about 0.25 diameters square; three set in line with the jet axis and three set inwards at 30° to the jet axis. A complete investigation of the corresponding reduction in mass flow was not made, but preliminary measurements indicated that the change was small. The maximum reduction in noise level was obtained with all the teeth pointing inwards. Some blockage did then occur and the results are therefore not quoted.

The optical investigation showed that the teeth deflected the flow inwards whilst the gaps between the teeth allowed an outflow. This resulted in a corrugation of the jet boundary. In an over-choked jet the corrugation of the jet boundary was still present but the shock pattern was diffused.

(d) The effect of the diffuser and slot

The results of a large number of tests, including the variation in slot width and diffuser angle, are given in Figure 41. The corresponding noise level curve for the unmodified jet (square end see Figure 6) is also included. The results showed some scatter but below choking no noise reduction occurred.

Above choking a reduction in the noise level was observed but this reduction was also present when the diffuser was removed ($h = \infty$), i.e. with the edge of the nozzle exit sharp. It appeared, therefore, that part of the high noise level obtained above choking with the unmodified nozzle was due to the blunt end at exit. It appears that a reduction of 3 db. approximately can be obtained with a sharp edged nozzle. The tests were, however, not conclusive and further investigation of this effect is necessary.

A large reduction in noise level was experienced when the nozzle end projected into the diffuser (see Figure 42). At $\mathcal{P} = 1.47$, with increase of pressure, a reduction in noise level of 11 db. was obtained but, with decrease of pressure, the corresponding increase in noise level did not occur until $\mathcal{P} = 1.26$. The reduction in noise level corresponded to a reattachment of the flow in the diffuser due to the expansion of the flow at the nozzle exit above choking. The flow in the diffuser was then supersonic and full expansion to atmospheric pressure took place. Below and just above choking breakaway of the flow in the diffuser was present.

7. DISCUSSION OF RESULTS

A. The distant noise field

It can be assumed that as $\tilde{\omega}/d$ approaches infinity the effect of the complete jet will be equivalent to that of a point sound radiator at the origin. The measurements in the distant field can, therefore, be applied to determine the characteristics of this point radiator and their variation with jet speed. It has been shown that the high frequency noise has a maximum intensity along lines at 45° to the jet axis. The lower frequencies do not exhibit a maximum along lines of 45° but since the measurements were made at only 108 diameters from the nozzle exit it is probable that asymptotic conditions were not reached.

The spectral density I_n, at high frequencies, follows, therefore, the asymptotic relation

$$I_n \sim \frac{x^2 r^2}{(x^2 + r^2)^3} . \qquad \ldots\ldots (7.1)$$

The total intensity contours do not show maxima along lines at 45° to the jet axis, but appear to be weighted by the low frequency spectrum. If the lateral

quadrupoles in Lighthill's theory[1] are at rest relative to the jet, the total intensity contours would indicate maxima along lines at 45° to the jet axis, but if they are in motion the angle for maximum intensity, relative to the jet axis, decreases as the relative speed increases. It appears, therefore, from the results above, that the low and high frequency sound radiators are moving at different speeds relative to the jet axis.

It is shown in Appendix 1 that at frequencies above 400 cycles per second the measurements of noise intensity follow approximately the relation

$$I_n \sim n^2 \, e^{-n^2/n^2_{max.}} \qquad \ldots\ldots (7.2)$$

where $n_{max.}$, the frequency for maximum intensity at any jet speed, appears to vary slightly with jet speed and θ.

On the basis of dimensional analysis the following laws for the total intensity and the spectral density at a point in the noise field have been obtained (see Appendix 2),

$$I_n \, dn = \frac{g(n,\theta)}{\tilde{\omega}^2} \, \rho^{b(n,\theta)} \, \rho_o \, d^5 \, dn \qquad \ldots\ldots (7.3)$$

$$I = \frac{h(\theta)}{\tilde{\omega}^2} \, \rho^{\bar{b}(\theta)} \, \rho_o \, d^2 \, a_o^3 . \qquad \ldots\ldots (7.4)$$

The values of $b(n,\theta)$, $\bar{b}(\theta)$, $g(n,\theta)$ and $h(\theta)$ determined from these tests are given in Tables 1 and 2.

The index $\bar{b}(\theta)$ varies for speeds just below choking from 4.0 inside the jet to 2.0 at about $\theta = 65^{\circ}$. Lighthill's theory suggests the value of 4.0 for all θ. At very low speeds $\bar{b}(\theta)$ approaches the value of 4.0, but at high speeds above choking it attains a value of about 8.5. The change in $\bar{b}(\theta)$ above choking appears to be connected with the shock pattern in the jet. When the shock train is eliminated (e.g. by the use of the gauze extension) it is possible to extend the unchoked pressure law to the case of the supersonic jet. It appears therefore that a value of $\bar{b}$ about 3.0 is associated with the noise produced by the turbulence in the mixing region.

Powell[5] has observed that ultrasonic waves* are emitted from an overchoked jet containing a train of shock waves, but there is evidence to show that this phenomenon is quite distinct from the creation of noise below choking.

---

*The jet diameter in Powell's experiment was 0.375 in. diameter. If the law $n_{max.} \sim a_o/d$ is correct, then the corresponding frequency in these tests would be 10,000 c/s. approximately.

It is possible, however, that the irregular results above $\rho = 1.3$, and in particular the 'whistle' obtained at $\theta = 30^{\circ}$, $\rho = 1.6$ (see Figure 15) at 10 kc/sec. may be due to the very high frequency waves of the type observed by Powell.

B. The near noise field

A full discussion of these results is given in Appendix 3 and only the salient remarks will be summarised here.

Although future investigations may throw light on how far the sound radiators created in the air jet retain their identity in motion down the jet, it is only possible, from the present measurements, to infer the distribution and strengths of the equivalent stationary sound radiators.

The high frequency noise radiators are distributed along the jet, near to the nozzle exit, for a distance which increases as the frequency decreases and is approximately proportional to the jet speed. The strength of the radiators reaches a maximum near the downstream end of their distribution along the axis.

It appears that the radiators behave like the lateral quadrupoles of Lighthill's theory although for the low frequency radiators the relatively long length of the jet along which they are distributed masks any directional effect which individual radiators may have and the evidence is therefore not conclusive.

The Lighthill theory also specifies a second lower maximum intensity along lines in the upstream direction at angles to the jet axis, which vary from 135° for a lateral quadrupole at rest, to about 115° when the quadrupole is moving at a Mach number of 0.9. The high frequency contours do show a second lower maxima between 90° and 110°, but there is no evidence of a second maxima in the contours for the total intensity.

It is very important to notice that the total intensity appears to be more heavily weighted by the lower frequencies at distances greater than 20 diameters from the nozzle exit. It is for this reason that past measurements have failed to reveal the marked directional character of the sound radiators.

C. The velocity distribution in the jet

It has been shown that the jet velocity in the direction of the axis has its major decrease in the region 4 to 25 diameters downstream of the nozzle exit. It has also been shown that the velocity gradient $(\partial U/\partial r)$ decreases rapidly with the distance downstream of the nozzle exit. These statements are very significant when it is remembered that the major distribution of the sound sources occurs in this same region.

D. The noise reduction devices

The object of these devices was to reduce the noise caused by the jets, bearing in mind their ultimate application to the jet units of aircraft*. The model tests were made to simulate the conditions of both the unchoked and the overchoked jet. Since the jet nozzle in the tests was stationary, the results may need modification when applied to flight conditions.

Of the various devices tested, it was found that the small teeth extensions (as used on the contraction sections of low speed open jet wind tunnels) in which half the total number of teeth pointed inwards whilst the remainder pointed along the jet axis, were the most satisfactory over the complete range of jet speeds above and below choking. The reduction in noise level was about 12 db. above and 5 db. below choking. It is suggested that the teeth could be incorporated in a device to vary the jet exit area.

The effect of the wire gauze extension in removing the shock pattern above choking is noteworthy apart from its sound reducing properties. A similar result should be obtained if it were fitted to a supersonic jet which emerged with excess static pressure.

The hysteresis effect obtained with the diffuser and slot is interesting but in view of its size, its possibilities are limited.

8. SUGGESTIONS FOR FUTURE EXPERIMENTAL RESEARCH WORK AND IMPROVEMENTS TO THE APPARATUS

Apparatus

(i) The Standard Telephone equipment is not satisfactory for this type of work. An instrument of greater precision is necessary including a filter which has a constant percentage band width over a frequency range of 10 cycles per second to 15 kilocycles per second.

(ii) A microphone of about 0.5 in. overall diameter and a flat response, from 10 c/s to 15 kc/sec., is necessary.

Experimental research work

(i) The measurements described in this report should be repeated using precise instruments on a carefully designed rig with a jet speed of about 300 f.p.s.

---

*It has been observed that the high frequency noise in a jet aircraft increases with altitude. If this effect is due to overchoking at the jet exit, the suggested noise reduction devices may be used to delay this increase.

(ii) The range of the low frequency measurements should be extended to investigate the directional characteristics of the low frequency sound radiators as well as the noise spectrum at these frequencies. The distant field measurements should not be made nearer than 500 jet diameters.

(iii) The measurements described in this report, of the noise level and spectrum, should also be made in the near and distant fields in the upstream direction.

(iv) The range of the high frequency measurements should be extended to above 10 kc./sec. in both the near and distant fields.

(v) The measurements described in this report should be repeated for jets at different temperatures.

(vi) The effect of the shape and edge thickness of the nozzle exit should be investigated further.

(vii) Measurements should be made of the turbulence intensity and correlations in the mixing region of an air jet to the vicinity of the jet exit. Measurements should also be made of the turbulence intensity and the mean velocity distribution of the transverse flow entering the jet mixing region.

(viii) The measurements described in this report should be repeated on jets of larger diameter.

9. SUGGESTIONS FOR FURTHER WORK ON THE NOISE REDUCTION DEVICES

(i) Teeth extensions should be fitted to jet engine test beds to find the best combination, giving maximum noise reduction, under all running conditions.

(ii) As a result of (i), teeth extensions should be fitted to the tail pipe of a jet aircraft and the measurements should include the internal cabin noise under flight conditions. Also observations should be made by ground observers during landing and take-off.

(iii) The use of the porous sleeve at the jet exit as a possible means of noise reduction on aircraft having supersonic jets should be investigated.

10. ACKNOWLEDGEMENTS

The authors wish to thank Professor A.D. Young who instigated this research and gave valuable advice at all stages in the investigation.

They also wish to acknowledge the help of Mr. E.G. Parkins and Mr. A. Peduzzi who assisted in setting up the apparatus and in the amassing of the experimental data, and they thank Mr. S.H. Lilley who was responsible for the construction of much of the apparatus and whose unfailing help was greatly appreciated.

They also wish to thank Mr. N. Fleming of the N.P.L. for the valuable assistance and advice he gave on numerous occasions during the investigation, and on whose unrivalled experience of the technique of noise measurement they were always able to draw.

Their thanks are due to the Director of the Royal Aircraft Establishment who kindly loaned the sound measuring equipment used in this investigation.

11. CONCLUSIONS

1. Measurements of the noise level and spectrum in the near and distant sound fields of a one inch diameter convergent nozzle at jet speeds above and below choking have shown that the elementary sound radiator (at least at high frequency) is a lateral acoustic quadrupole. This result is in agreement with Lighthill's theory of jet noise.

2. The high frequency noise radiators are distributed along the jet, near to the nozzle exit, for a distance which increases as the frequency decreases and is approximately proportional to the jet speed. The strength of the radiator reaches a maximum near the downstream end of their distribution along the axis.

3. An empirical formula is presented for the determination of noise intensity at a given position from the nozzle exit outside the jet.

4. Various noise reduction devices have been tested. Small teeth extensions, which caused only very slight jet blockage, produced reductions in noise level of 5 db. and 12 db. below and above choking respectively.

REFERENCES

No.	Author	Title, etc.
1.	Lighthill, M.J.	On Sound Generated Aerodynamically. Part I - General Theory. A.R.C. 14,407. F.M.1630 (1951).
2.	Billing, H.	Sources of Sound in Motion. A.V.A. Monograph R and T 960 (1947).
3.	Batchelor, G.K.	Pressure Fluctuations in Isotropic Turbulence. Proc. Cam. Phil. Soc. Vol.47, pt.2, pp.359-374 (1951).
4.	Schwarzschild	Zeeman Shifts for Stellar Dipoles and Quadrupoles with Inclined Axis. Astrophysics Journal Vol.112, p. 222 (1950).
5.	Powell, A.	Some Experimental Observations on the Behaviour of Free Air Jets. University College, Southampton Research Note (1951).
6.	Lilley, G.M.	Some theoretical Aspects of Nozzle Design. London University M.Sc. Thesis (1945).
7.	Townsend, A.A.	Measurements in the Turbulent Wake of a Cylinder. Proc. Roy. Soc. A.190, p.551 (1947).
8.	Corrsin, S.	Investigation of the Flow in an Axially Symmetrical Heated Jet of Air. NACA ACR 3L23 (1943).
9.	Townsend, A.A.	Momentum and Energy Diffusion in the Turbulent Wake of a Cylinder. Proc. Roy. Soc. A.197, p.124 (1949).
10.	Goldstein, S. (editor)	Modern Developments in Fluid Dynamics. Vol.I, p.288 (1938).

A P P E N D I X I

The Variation of Noise Level with Frequency

In these tests the noise spectrum has been measured in octave bands. If the band widths are

$$(2n_1 - n_1),\quad (4n_1 - 2n_1),\quad (8n_1 - 4n_1) \ldots\ldots (2mn_1 - mn_1),$$

then if $I_n dn$ is the intensity of noise in a band width dn at a frequency n, the total intensity I is given by

$$I = \int_0^{\infty} I_n dn = \int_0^{n_1} I_n dn + \int_{n_1}^{2n_1} I_n dn + \ldots\ldots \int_{mn_1}^{2mn_1} I_n dn + \int_{2mn_1}^{\infty} I_n dn$$

$$= I_o + I_1 + I_2 + \ldots\ldots + I_m + I_{\infty} \qquad \ldots\ldots (A.1)$$

where

$$I_o = \int_0^{n_1} I_n dn$$

$$I_1 = \int_{n_1}^{2n_1} I_n dn$$

$$I_m = \int_{mn_1}^{2mn_1} I_n dn$$

$$I_{\infty} = \int_{2mn_1}^{\infty} I_n dn$$

are the noise intensities in the various octaves.

But the total noise level is given in the form

$$N(db) = 10 \log_{10} \frac{I}{I_{th}} \qquad \ldots\ldots (A.2)$$

and the octave noise level

$$N_{\alpha} = 10 \log_{10} \frac{I_{\alpha}}{I_{th}} . \qquad \ldots\ldots (A.3)$$

Hence

$$\frac{I_{\alpha}}{I_{th}} = 10^{\left(\frac{N_{\alpha}}{10}\right)} \qquad \ldots\ldots (A.4)$$

and the mean intensity per cycle in this octave of band width αn_1 is,

$$\bar{I}_\alpha = \frac{I_\alpha}{\alpha n_1} . \qquad \ldots\ldots (A.5)$$

If further

$$I_n = f(U,d,\underline{x},\rho_o,a_o)\ n^2\ F(n) \qquad \ldots\ldots (A.6)$$

then

$$I = f \int_0^\infty n^2\ F(n)\ dn \qquad \ldots\ldots (A.7)$$

and from equations (A.1) and (A.5) at some position in the band of width αn_1

$$\bar{I}_\alpha = f\ n^2\ F(n) \qquad \ldots\ldots (A.8)$$

or

$$10 \log_{10} \frac{\bar{I}_\alpha}{I_{th}} = 10 \log_{10} \frac{f}{I_{th}} + 10 \log_{10} n^2 F(n) \ldots\ldots (A.9)$$

The values of $10 \log_{10} \frac{\bar{I}_\alpha}{I_{th}}$ has been plotted against log n in Figure 43 for the case $\theta = 45^o$, $\mathcal{P} = 0.9$ and $\tilde{\omega}/d = 108$. Similar curves can be plotted for all other conditions. It is shown that in the frequency range 400 to 10,000 c/s

$$F(n) \triangleq e^{-n^2/n^2_{max.}} \qquad \ldots\ldots (A.10)$$

where $n_{max.}$ is the frequency for maximum intensity at any given jet speed. F(n) is a function of θ and varies slightly with jet speed.

The test results show that at $\mathcal{P} = 0.9$, in the frequency range 30 to 300 c/s, the noise is 'white'*, but, as stated above, the readings are probably incorrect owing to filter leakage. At lower jet speeds the energy in each of the lower octaves falls with frequency and the spectral density is approximately constant. It is still probable, however, that these readings, in the octave bands below 14, are incorrect. It is therefore necessary to make more accurate observations and to check whether the above law is verified at the lower frequencies.

---

*The noise is 'white' when the energy in each octave is approximately constant.

Finally, it should be noted that if

$$I_n \sim n^c \qquad \ldots\ldots (A.11)$$

the intensity I_α in a band of frequency between αn_1 and $2\alpha n_1$ is given by

$$I_\alpha \sim (\alpha n_1)^{c+1} . \qquad \ldots\ldots (A.12)$$

This explains why the frequency spectra at different jet speeds in Figures 19-23 obey the law

$$\frac{I_\alpha}{I_{th}} \left(= 10^{N_\alpha/10} \right) \sim n^3 \qquad \ldots\ldots (A.13)$$

in the band 400 to 2000 cycles per second.

A P P E N D I X II

A General Formula for the Noise Intensity from a Jet

Let the spectral density

$$I_n = f(\tilde{\omega},\ \theta,\ \rho_o,\ a_o,\ \Delta p,\ d,\ n,\ n_{max.}) \qquad \ldots\ldots (A2.1)$$

where $\Delta p = p_s - p_o$.

Since I has the dimensions Mass/(Time)^3 the spectral density will have the dimensions Mass/(Time)^2.

The Π theorem tells us that we can select six independent non-dimensional groups from inspection of equation (A2.1) and these groups must be related.

Thus we can write

$$\frac{I_n}{\rho_o d a_o^2} \sim f\left(\theta,\ \frac{\tilde{\omega}}{d},\ \frac{\Delta p}{\rho_o a_o^2},\ \frac{nd}{a_o},\ \frac{n}{n_{max.}}\right) \qquad \ldots\ldots (A2.2)$$

and we will assume the form

$$I_n \sim g(\theta) \left(\frac{\tilde{\omega}}{d}\right)^{\beta_1} \left(\frac{\Delta p}{\rho_o a_o^2}\right)^{\beta_2} \left(\frac{nd}{a_o}\right)^{\beta_3} F\left(\frac{n}{n_{max.}}\right) \rho_o a_o^2 d \,. \qquad \ldots\ldots (A2.3)$$

Since $p_o \sim \rho_o a_o^2$ we can write, in place of $\Delta p/\rho_o a_o^2$, $\Delta p/p_o = \mathcal{P}$.

We can further assume a slight dependence of all quantities on the Reynolds Number $\rho_1 U_1 d/\mu_1$.

Similarly the expression for total noise is

$$I \sim h(\theta) \left(\frac{\tilde{\omega}}{d}\right)^{\beta_1} \left(\frac{\Delta p}{\rho_o a_o^2}\right)^{\beta_2} \rho_o a_o^3 \,. \qquad \ldots\ldots (A2.4)$$

The distant field measurements for high frequencies have shown that $\beta_1 = -2$

$$\beta_3 = 2$$

and $$F\left(\frac{n}{n_{max.}}\right) = e^{-n^2/n^2_{max.}}.$$

With these values

$$I_n dn = \frac{g(\theta)}{\tilde{\omega}^2} n^2 e^{-n^2/n^2_{max.}} \mathcal{P}^{\beta_2} \rho_o d^5 dn \qquad \ldots\ldots (A2.5)$$

and

$$I = \frac{h(\theta)}{\tilde{\omega}^2} \mathcal{P}^{\beta_2} \rho_o a_o^3 d^2 \qquad \ldots\ldots (A2.6)$$

where

$$\frac{g(\theta)}{\tilde{\omega}^2} \sim \frac{x^2 r^2}{(x^2 + r^2)^3} . \qquad \ldots\ldots (A2.7)$$

It has been observed that the relation (A2.7) describes the noise field of the jet if a suitably chosen origin is taken. This origin should coincide presumably with the centre of the sound radiator, and an equation such as (A2.5) would then describe the intensity outside the jet due to a single sound radiator.

Below choking, the value of β_2 varies from 3.8 to 2.0 in the range. $30^o < \theta < 90^o$. The apparatus was such that the value of β_2 could not be obtained accurately at low speeds, but the evidence indicates that at these speeds β_2 is of the order 4. This is the value suggested by Lighthill on the basis of his theory.

If we integrate equation (A2.5) with respect to n between the limits of zero and infinity and then compare the result with equation (A2.6), it can be shown that

$$n_{max.} \sim \frac{a_o}{d} \ell(\theta). \qquad \ldots\ldots (A2.8)$$

The relation (A2.8) may prove important in the determination of changes in the frequency spectrum at larger jet diameters. It should be noted that the effect of temperature variations in the jet has not been investigated in these tests. They may be important.

A P P E N D I X III

The Sound Field due to a Quadrupole and Verification of its Existence in the Jet both Above and Below Choking

Lighthill[1] has determined that the intensity at ($\underline{x}$) due to a point quadrupole at rest situated at the origin, is given by

$$I \sim \frac{x^2 r^2}{(x^2 + r^2)^3} . \qquad \ldots\ldots (A3.1)$$

The sound field, in one quadrant only, is plotted in Figure 44.

The locus of points, on the constant intensity lines for which dr/dx is equal to zero, is a line defined by $\tan \theta_1 = 1/\sqrt{2}$ or $\theta_1 \triangleq 35\ 1/4^\circ$. The locus of points, on the constant intensity lines for which dr/dx is infinite, is a line defined by $\tan \theta_2 = \sqrt{2}$ or $\theta_2 \triangleq 54\ 3/4^\circ$. The line drawn through the points of maximum noise intensity is at the angle $\theta_m = 45^\circ$ to the axis.

The sound field contour diagrams in Figures 24 to 33 have been plotted in steps of 1 db. If the sound radiator is a quadrupole then, on a line at 45° to the jet axis and passing through the radiator, adjacent contour lines should be at radial distances in the ratio

$$\sqrt{\text{Antilog}_{10}\ 0.1} : 1 \qquad \text{or} \qquad 1.122 : 1.$$

In Figures 25 to 28 inclusive for $\mathcal{P} = 0.9$ and at the higher frequencies, it can be seen that the contour lines surrounding the downstream limit of the sound source distribution in the jet closely resemble the contours shown in Figure 44. The lines corresponding to the maximum intensity, viz. θ_m, and the lines corresponding to the locus of points on the constant intensity lines for which dr/dx = 0 and ∞, viz. θ_1 and θ_2 respectively, are drawn on these diagrams. These lines show good agreement with those corresponding to a quadrupole field, viz. $\theta_m = 45^\circ$, $\theta_1 \triangleq 35\ 1/4^\circ$ and $\theta_2 \triangleq 54\ 3/4^\circ$. The radial distance ratio of 1.122 : 1 on the lines of maximum intensity, which is a requirement of the quadrupole field, does not in all cases equal the measured values, but in view of the very great difficulty experienced in taking measurements, this slight disagreement is not considered important.

Likewise in Figure 32, for $\mathcal{P}$ = 1.33, similar agreement with the simple quadrupole field is obtained even though in this case shock waves are present in the jet.

These results indicate that stationary distributions of sound sources, not necessarily continuous, exist at various positions in the jet. These sound sources have the directional properties of a lateral acoustic quadrupole. It is very necessary to point out, however, that these tests have not shown in all cases a second lower maximum noise intensity in the upstream region from the nozzle exit, which is an essential requirement of the quadrupole theory. It has been suggested that the jet nozzle will prevent this by obstructing the upstream direction. This suggestion appears unlikely except for the noise produced very close to the nozzle exit. It is possible, however, that the cause of this disagreement lies in the high speed of the jet whose upstream and downstream sound radiation are respectively decreased and increased as compared with a low speed jet. This suggested explanation appears to be the more likely one, since measurements below choking show that large changes in the noise field occur as the jet speed is increased (see Figure 18).

The measurements show that the extent of the sound source distribution is a function of the jet speed and frequency. It appears that the complete sound source distribution is close to the nozzle exit only at very low jet speeds and at the high frequency. Although Figures 25 to 28 and 32, for the high frequency, show that the sound radiators, at least at the downstream end of their distribution, have the properties of lateral acoustic quadrupoles at rest, there is no direct evidence to show that these properties are also possessed by the low frequency sound radiators (see Figures 29 to 31 and 33).

These measurements cannot be used to predict accurately the characteristics of moving sound radiators in the jet (if indeed these are present) since the microphone readings give the mean sound intensity only over a long period of time compared with the characteristic time of the eddies responsible, presumably, for the phenomenon of noise. These results show (see Figures 25-28) that, at high jet speeds, the high frequency sound radiators exist in the region between the nozzle exit and 15 diameters downstream. The strength of these radiators reaches a maximum near the downstream end of their distribution. The low frequency sound radiators (see Figures 29 and 30), on the other hand, appear to be distributed over much greater lengths of the jet, but they still exhibit this characteristic maximum radiation of noise near the downstream end of their distribution.

One important feature of the experiments should be noted which, if later verified, may prove to play a very important part in the explanation of this phenomenon. It was noticed that when noise measurements were made using a wave analyser having a relatively small band width, the readings displayed an irregular intermittency of the type already

recorded by Townsend[7] and Corrsin[8] in measurements on free turbulent shear flow in wakes and jets respectively. This intermittency has been explained by Townsend[9] as being due to the irregular boundary between the jet and the undisturbed flow outside, (see, for example, Plate 24b of reference 10), which is caused by the billows of turbulent fluid moving outwards from the turbulent mixing region. These jets of turbulent fluid are probably large eddies which carry smaller eddies in dynamic equilibrium with each other. From the measurements of the noise frequency spectrum, it is evident that the small eddies, having high intensity and producing the high frequency noise, are confined to the regions close to the nozzle exit. On the other hand, since the large eddies, having high intensity, exist over much greater lengths of the jet, it might be expected that the corresponding output of low frequency noise is not restricted to relatively small volumes of the jet.

T A B L E I

Values of $b(n,\theta)$ and $\bar{b}(\theta)$

for the distant noise field $\tilde{\omega}/d > 50$, jet temperature equal to atmospheric temperature and $\mathcal{P} \leq 1$.

Notation

$(\tilde{\omega},\theta)$ Spherical polar coordinates with the jet exit as origin and the jet axis as datum.

n Frequency.

d Jet exit diameter.

a_o Speed of sound in the atmosphere.

	$b(n,\theta)$					$\bar{b}(\theta)$
$\frac{nd}{a_o}$ / θ^o	0.0325 — 0.065	0.065 — 0.130	0.130 — 0.260	0.260 — 0.520	0.520 — 1.040	Total
30^o	3.00	3.18	3.37	3.56	3.75	3.34
45^o	2.43	2.54	2.66	2.78	2.90	2.66
60^o	2.13	2.19	2.24	2.30	2.36	2.26
75^o	2.13	2.14	2.16	2.17	2.19	2.15
90^o	2.40	2.47	2.52	2.59	2.65	2.56

T A B L E II

Values of $g(n,\theta)$ and $h(\theta)$

for the distant noise field $\tilde{\omega}/d > 50$, jet temperature equal to atmospheric temperature and $\rho \leq 1$.

$$I_n dn = \frac{g(n,\theta)}{\tilde{\omega}^2} \rho^{b(n,\theta)} \rho_o d^5 dn \quad , \text{ see equation (7.3)}$$

$$I = \frac{h(\theta)}{\tilde{\omega}^2} \rho^{\bar{b}(\theta)} \rho_o d^2 a_o^3 \quad , \text{ see equation (7.4)}$$

Units

Mass - slug

Length - foot

Time - second.

In these units I is measured in ft.lb./ft^2/sec. and the threshold intensity I_{th} (10^{-16} watts per sq.cm.) is equal to 685.0×10^{-16} ft.lb./ft^2/sec.

	$g(n,\theta)$					$h(\theta)$
$\frac{nd}{a_o}$ / θ^o	0.0325 — 0.065	0.065 — 0.130	0.130 — 0.260	0.260 — 0.520	0.520 — 1.040	Total
30^o	1590.	8300.	8900.	1400.	150.	9.34×10^{-6}
45^o	170.	950.	4500.	1900.	260.	5.37
60^o	90.	360.	1300.	600.	240.	1.86
75^o	70.	250.	660.	400.	170.	1.18
90^o	60.	170.	320.	330.	80.	0.71

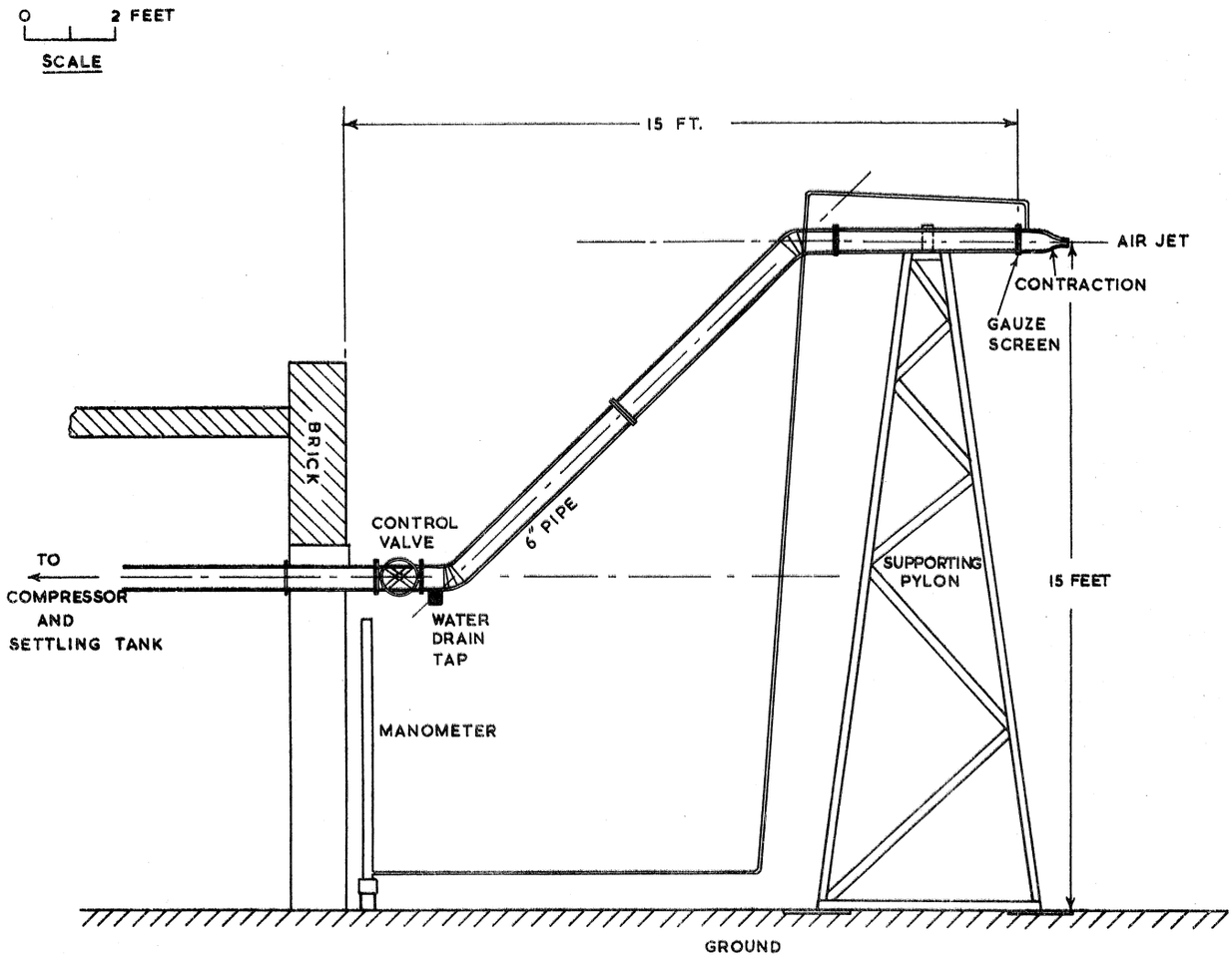

FIG. 1. SIDE ELEVATION OF THE AIR JET.

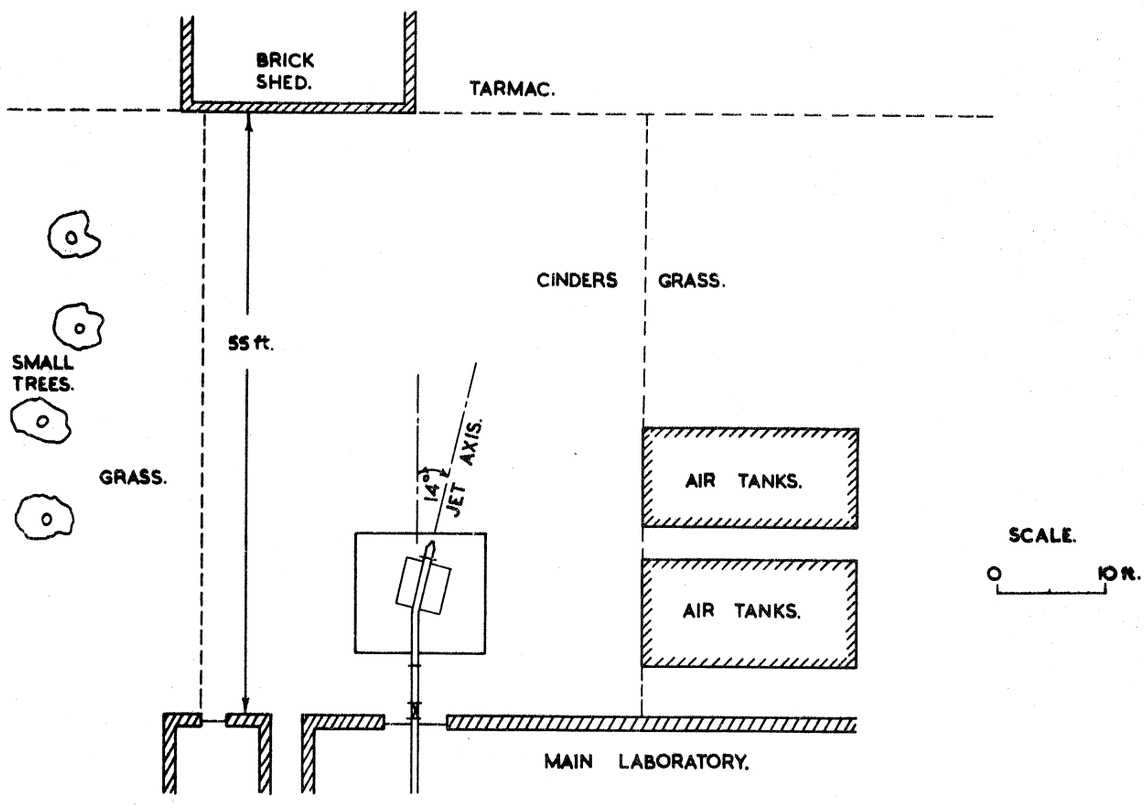

FIG. 2. PLAN VIEW OF THE JET SITE.

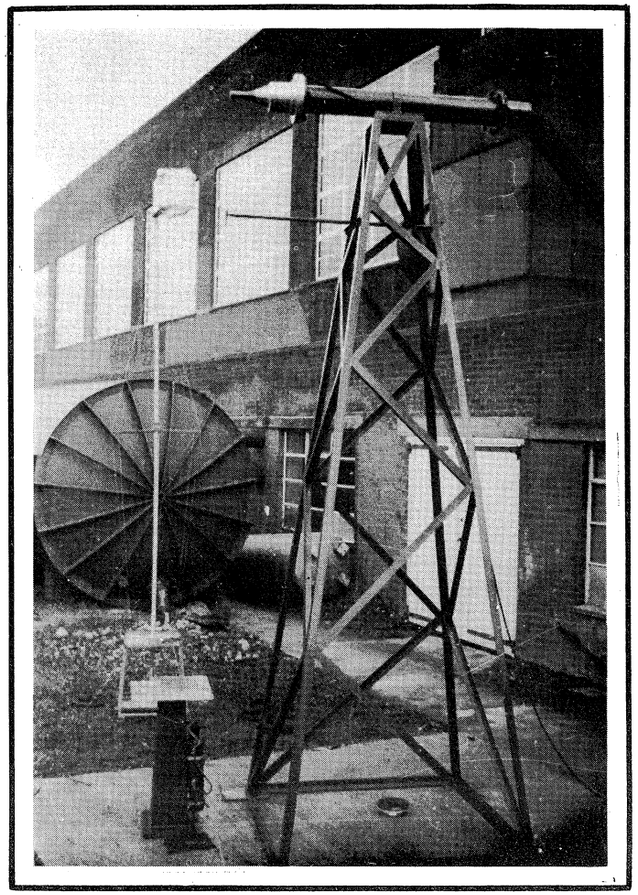

FIG. 3.

SIDE VIEW OF THE JET

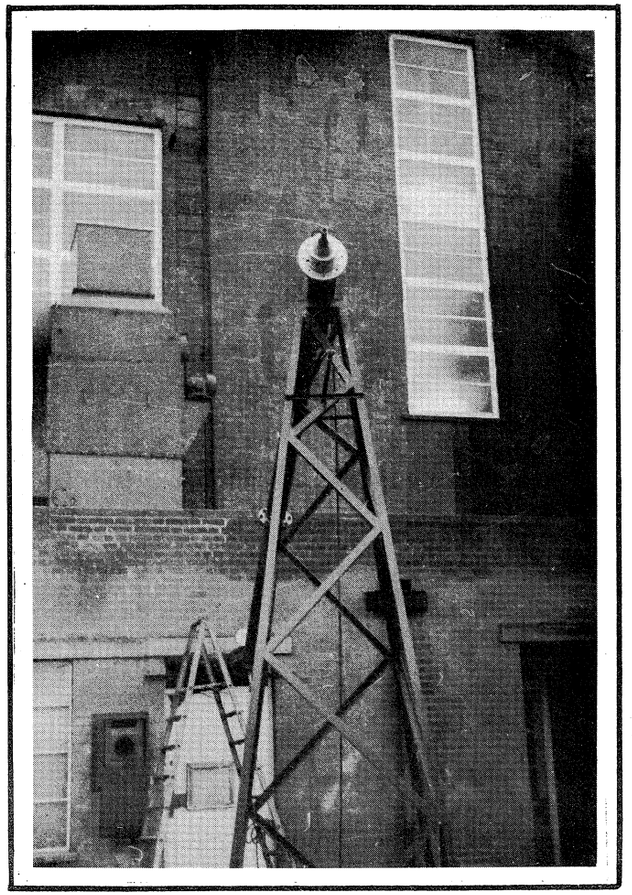

FIG. 4.

END VIEW OF THE JET

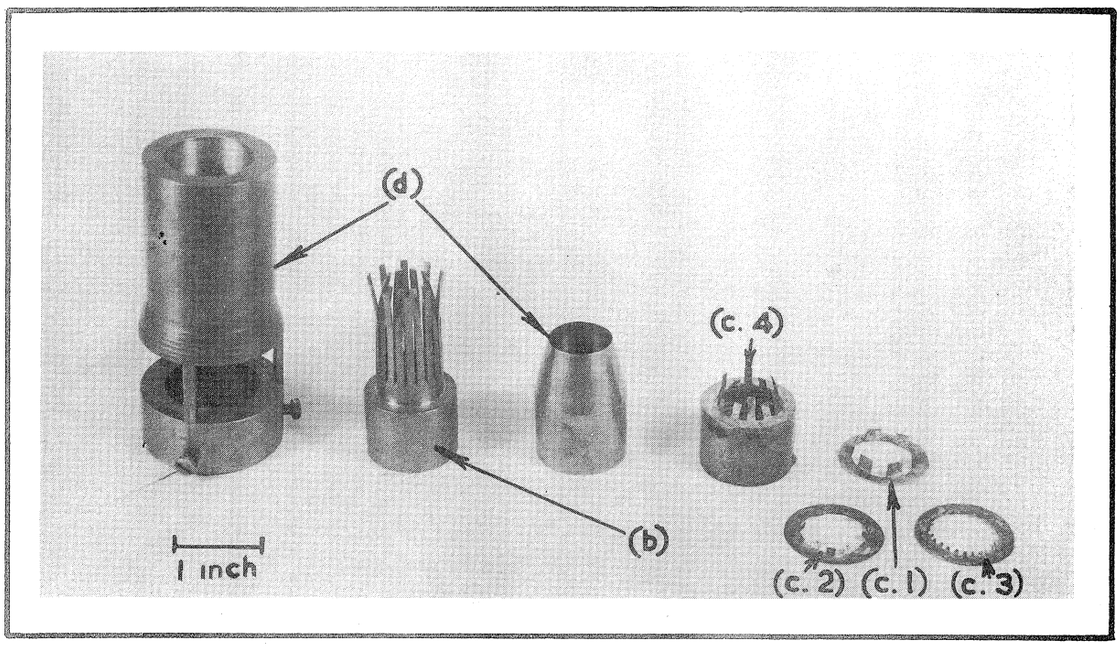

FIG. 5.

THE NOISE REDUCTION DEVICES

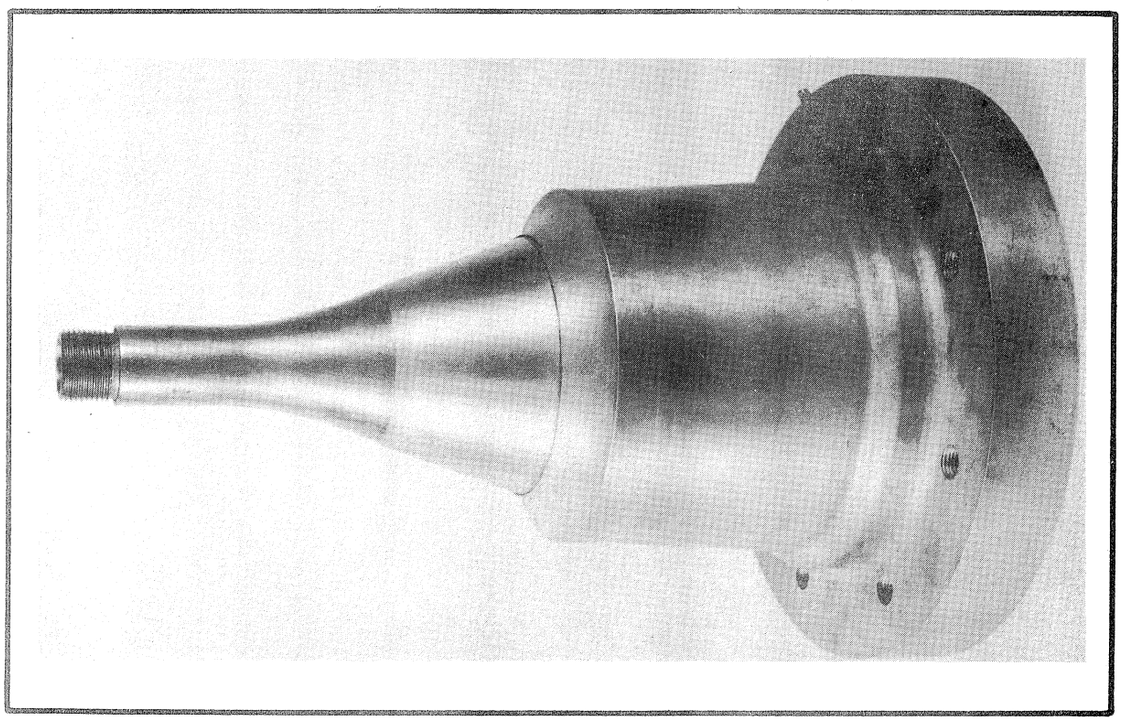

FIG. 6.

THE CONTRACTION AND NOZZLE EXIT.

(NOTE: The internal contour does not follow the external lines.)

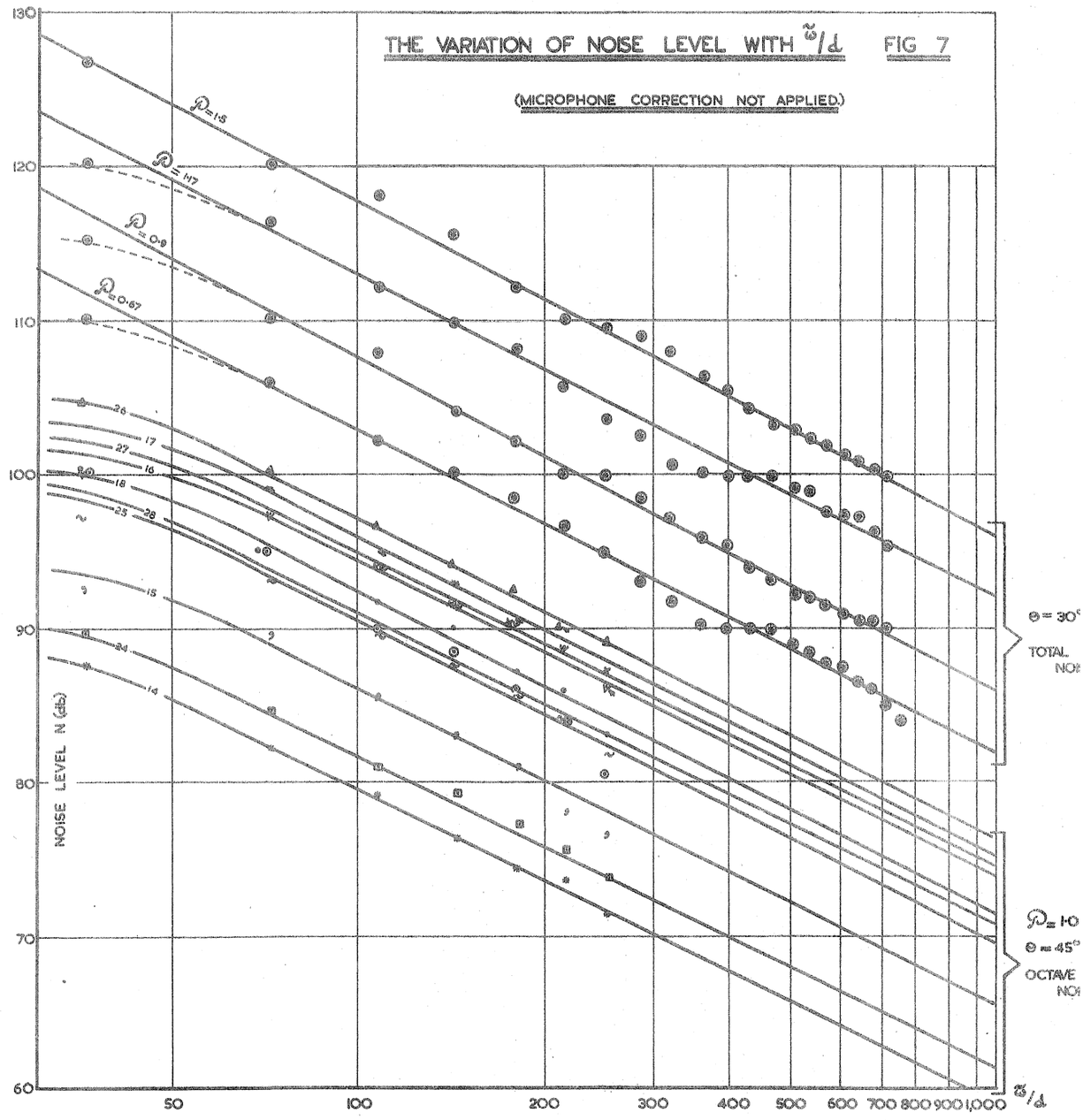

FIG 7

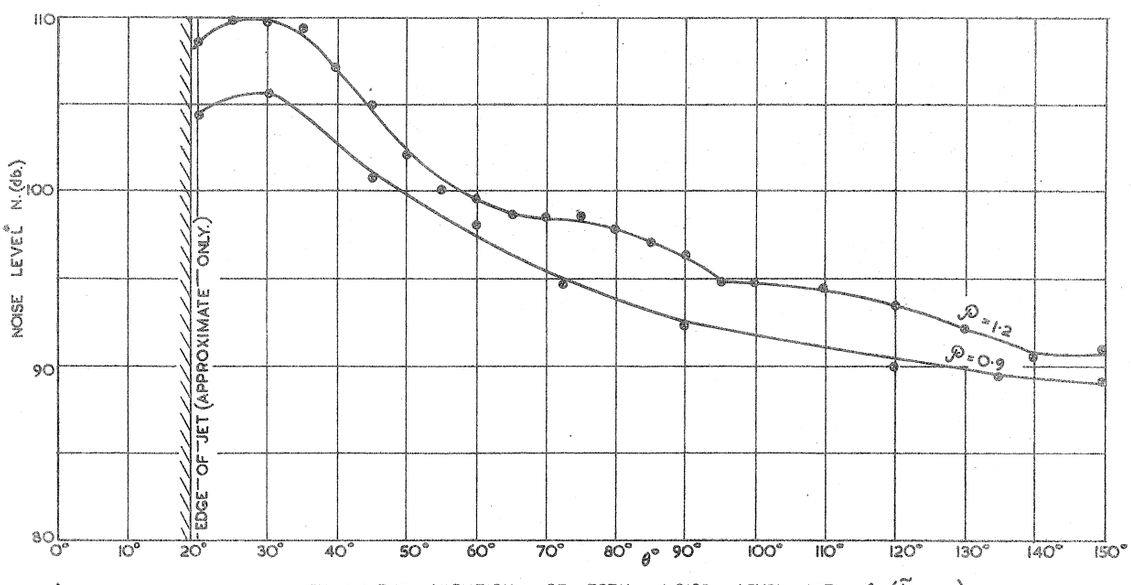

FIG. 8. THE VARIATION OF TOTAL NOISE LEVEL WITH θ ($\frac{\tilde{\omega}}{d}$=108.)
(MICROPHONE CORRECTION NOT APPLIED.)

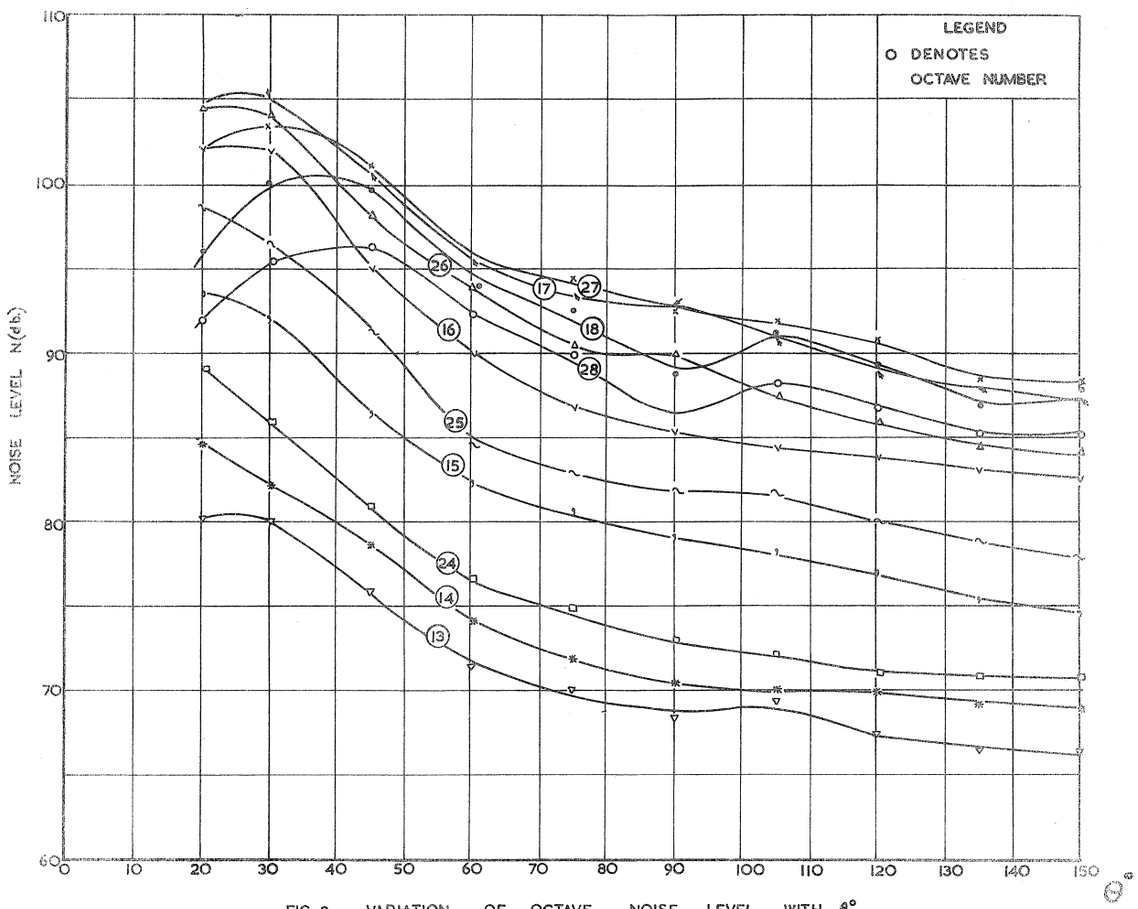

FIG. 9. VARIATION OF OCTAVE NOISE LEVEL WITH θ°
(MICROPHONE CORRECTION APPLIED.)
$\mathcal{D} = 0{\cdot}9$ $\frac{\omega}{a} = 108.$

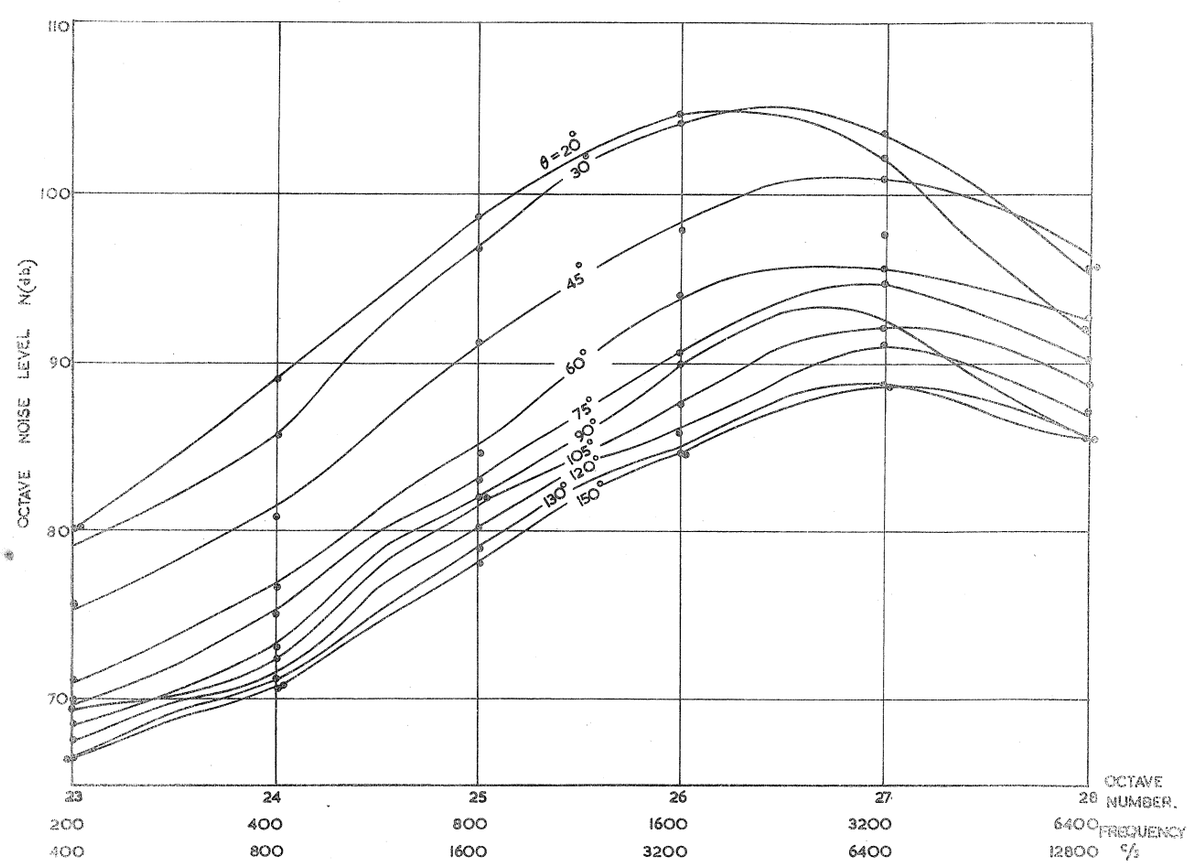

FIG. 10. THE VARIATION OF NOISE LEVEL WITH FREQUENCY.
(MICROPHONE CORRECTION APPLIED.)
$\mathcal{D} = 0{\cdot}9$ $\frac{\omega}{a} = 108$

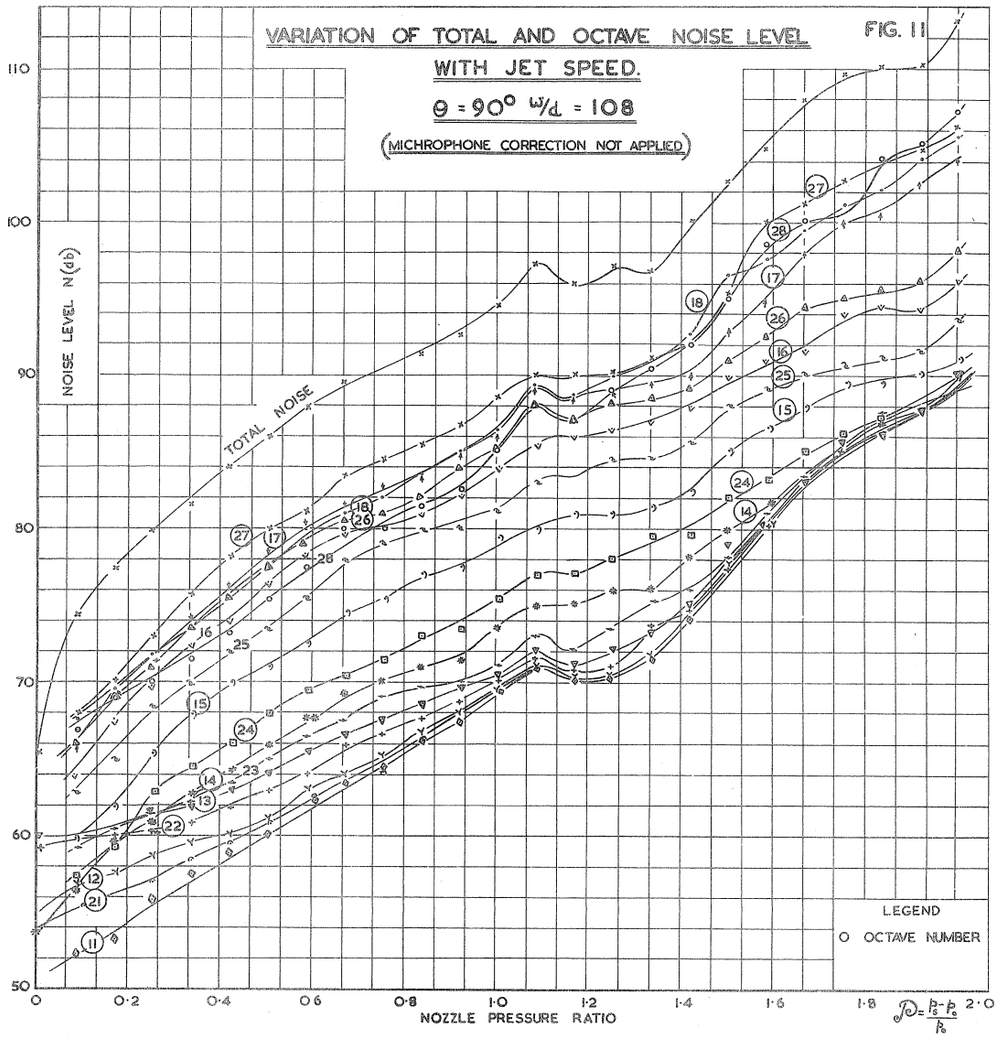

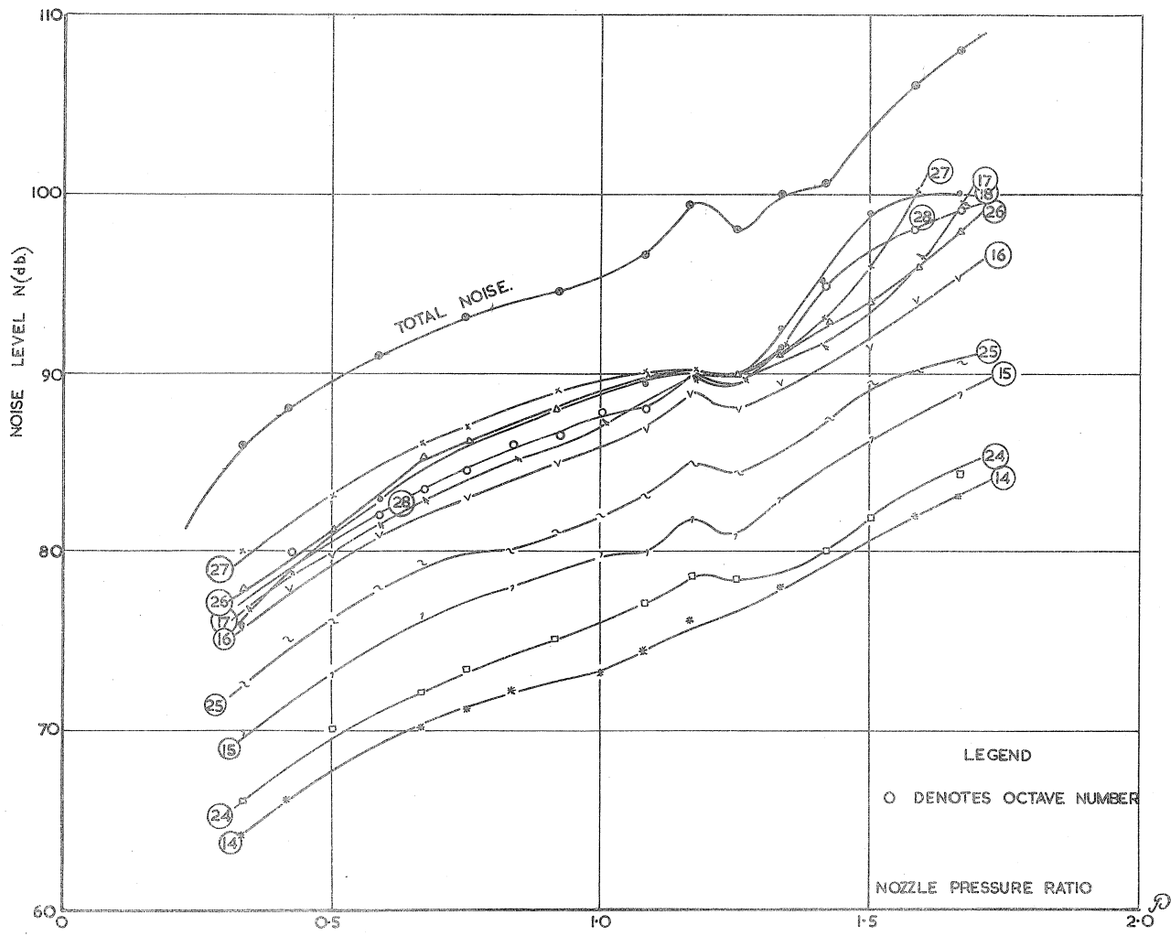

FIG. 12. VARIATION OF TOTAL AND OCTAVE NOISE LEVEL WITH JET SPEED.
(MICROPHONE CORRECTION NOT APPLIED.)
$\theta = 75^\circ$ $\frac{w}{d} = 108$.

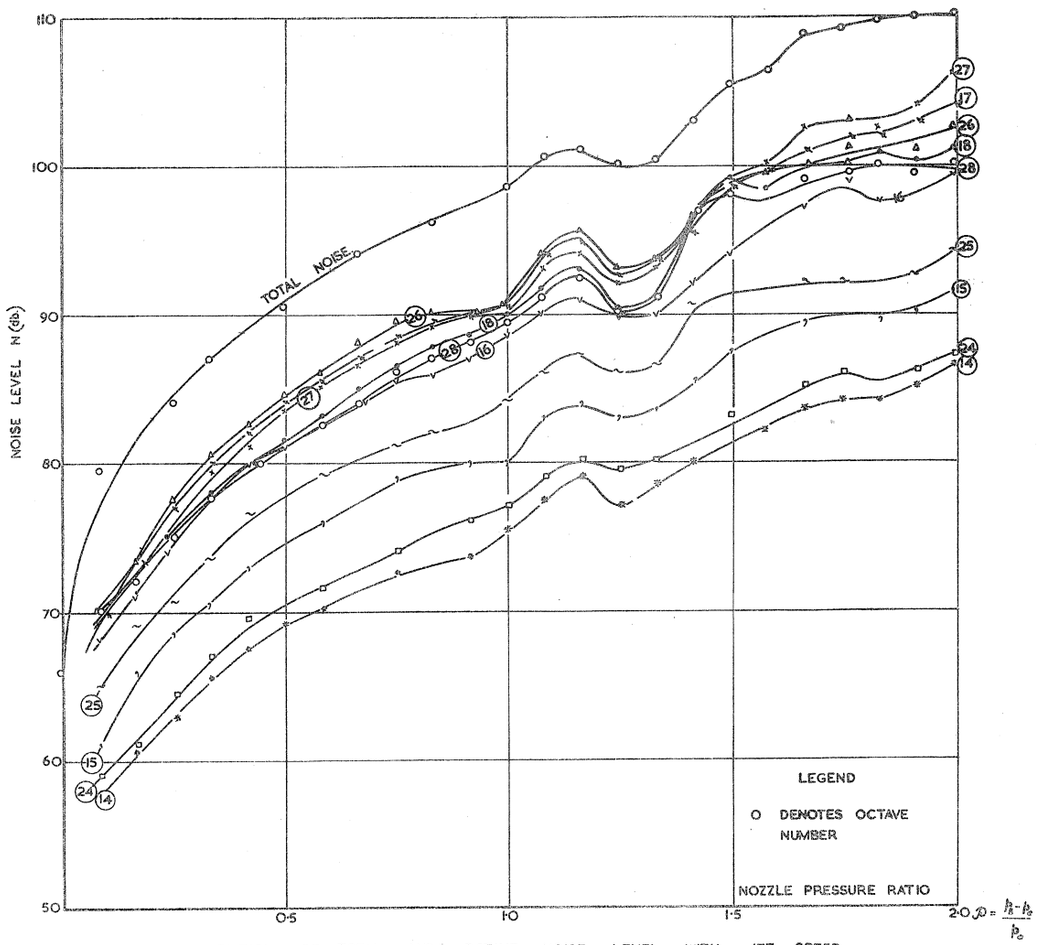

FIG. 13. VARIATION OF TOTAL AND OCTAVE NOISE LEVEL WITH JET SPEED
(MICROPHONE CORRECTION NOT APPLIED.)
$\theta = 60°$ $\frac{D}{d} = 108.$

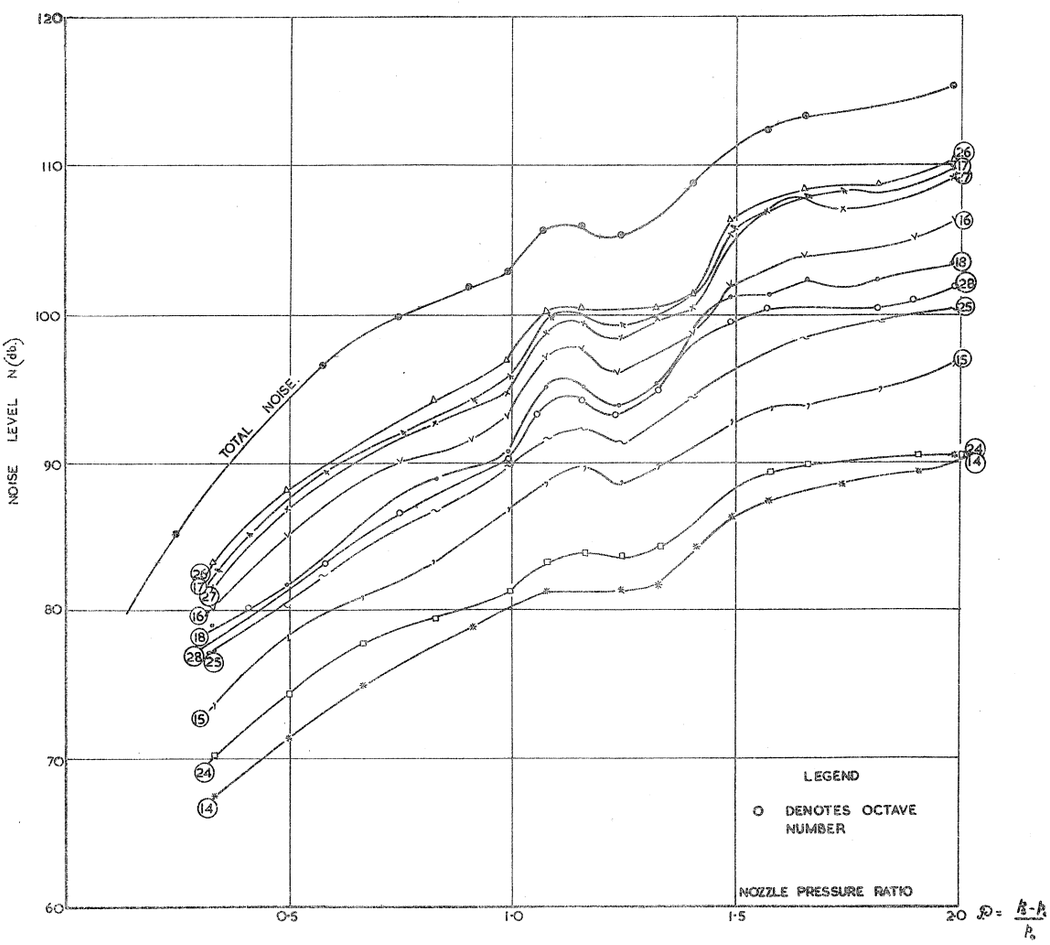

FIG. 14. VARIATION OF TOTAL AND OCTAVE NOISE LEVEL WITH JET SPEED.
(MICROPHONE CORRECTION NOT APPLIED.)
$\theta = 45°$ $\frac{D}{d} = 108.$

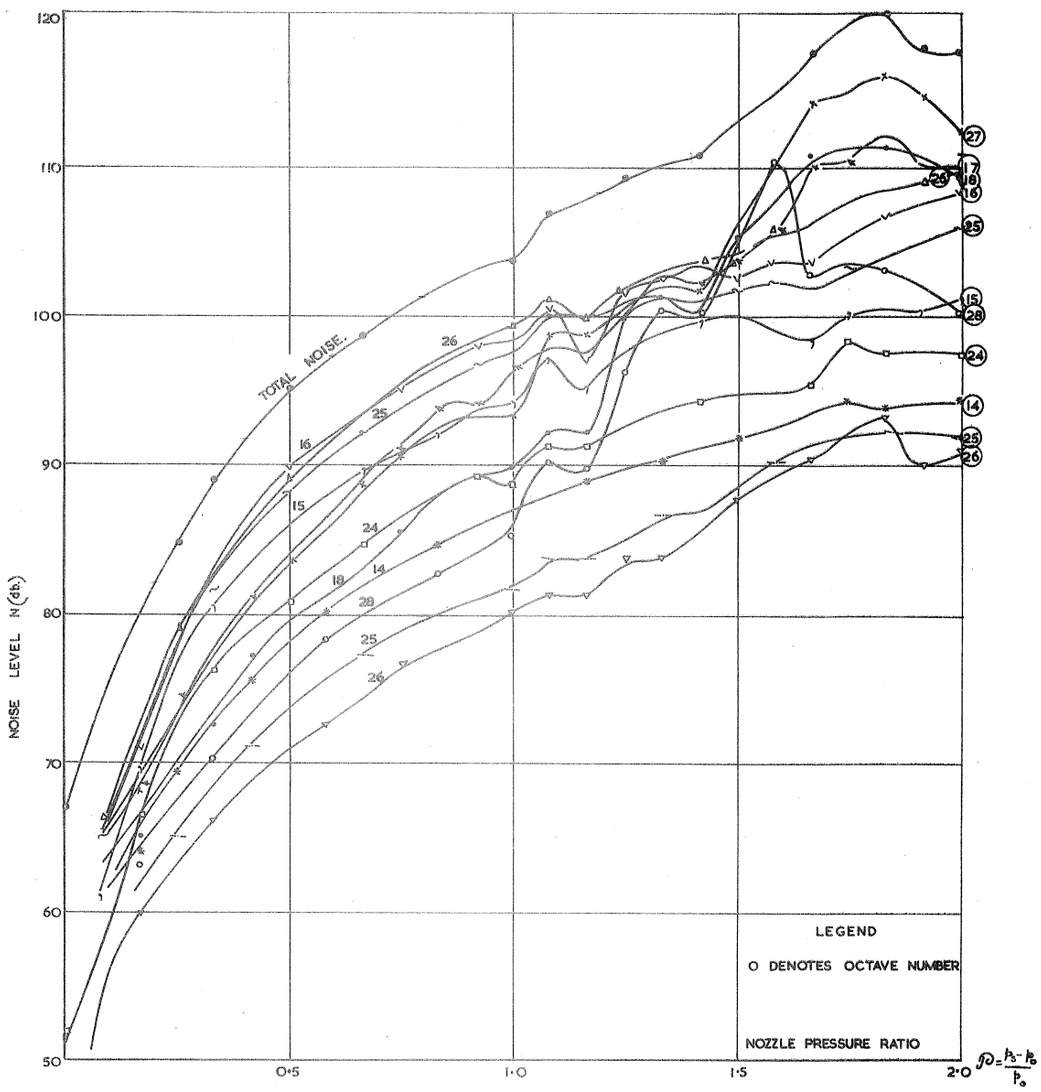

FIG. 15. VARIATION OF TOTAL AND OCTAVE NOISE LEVEL WITH JET SPEED (MICROPHONE CORRECTION NOT APPLIED.)
$\theta = 30°$. $\frac{2l}{d} = 108$.

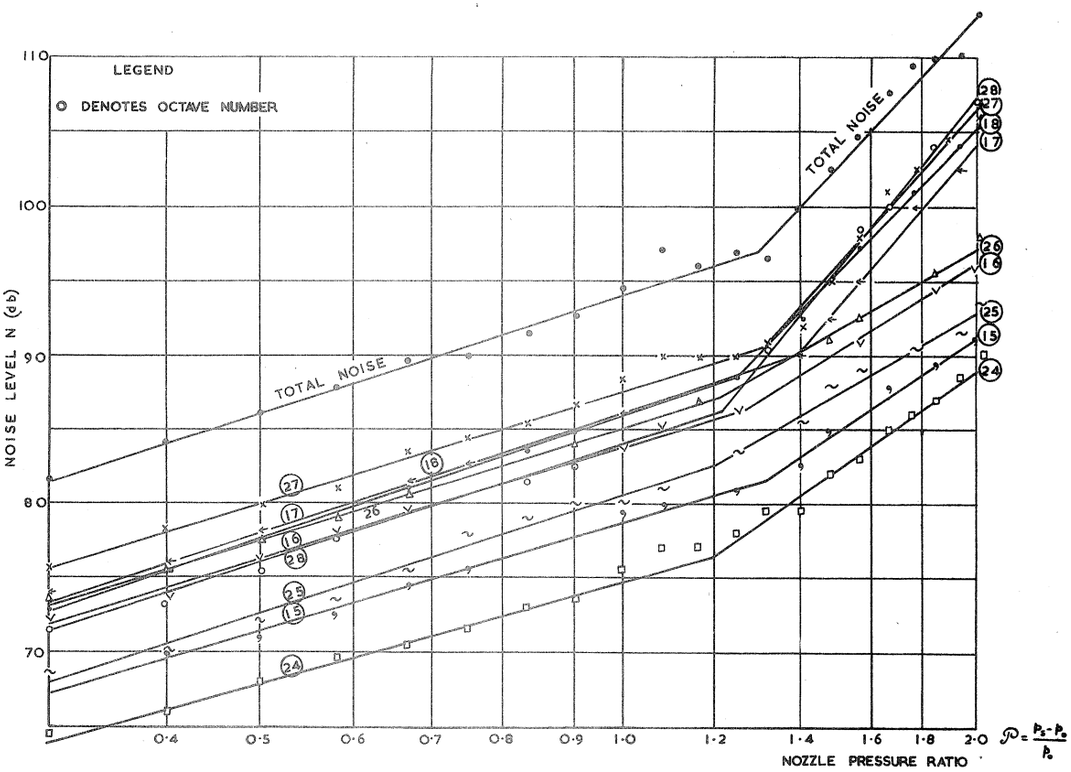

FIG. 16. RATE OF INCREASE OF NOISE LEVEL WITH JET SPEED. $\theta=90°$ $\frac{2l}{d}=108$. (NO MICROPHONE CORRECTION APPLIED.)

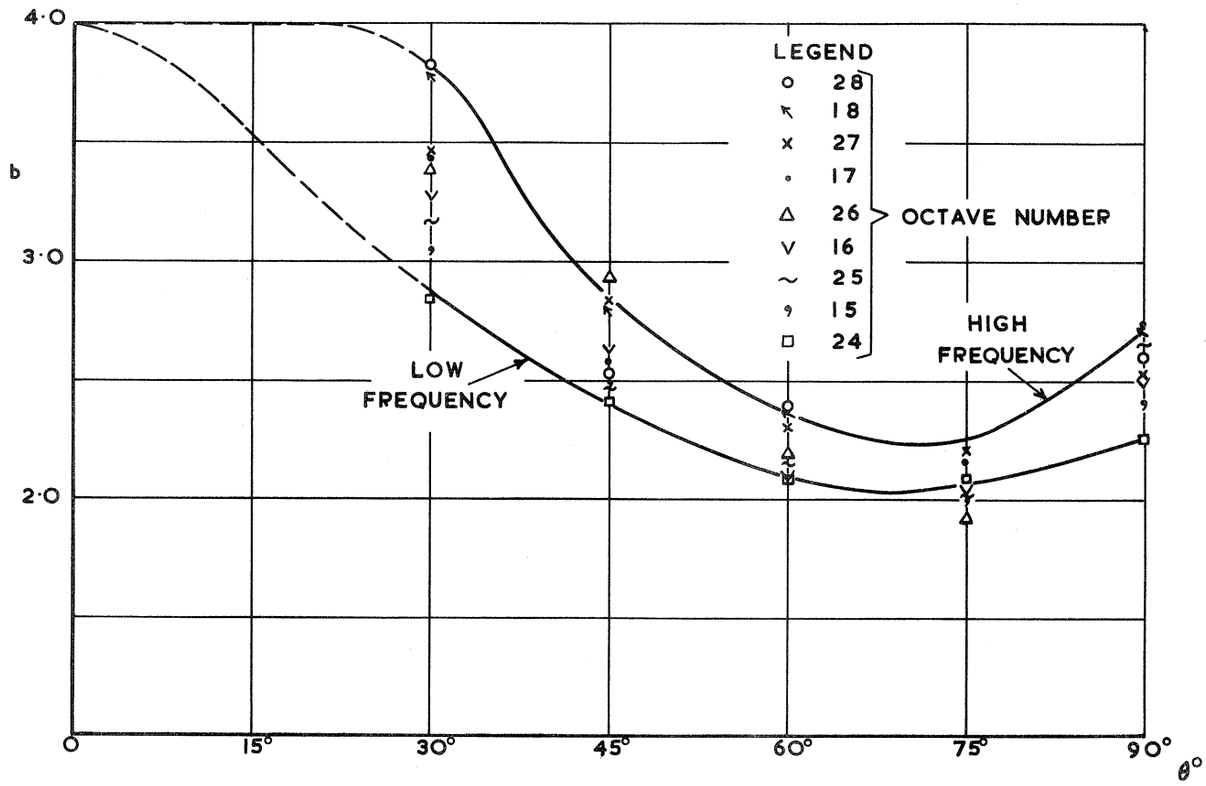

FIG 17. VARIATION OF THE INDEX b WITH θ° WHERE $I_n \sim \mathcal{P}^{b(\theta)}$ $\frac{\tilde{\omega}}{d} = 108$

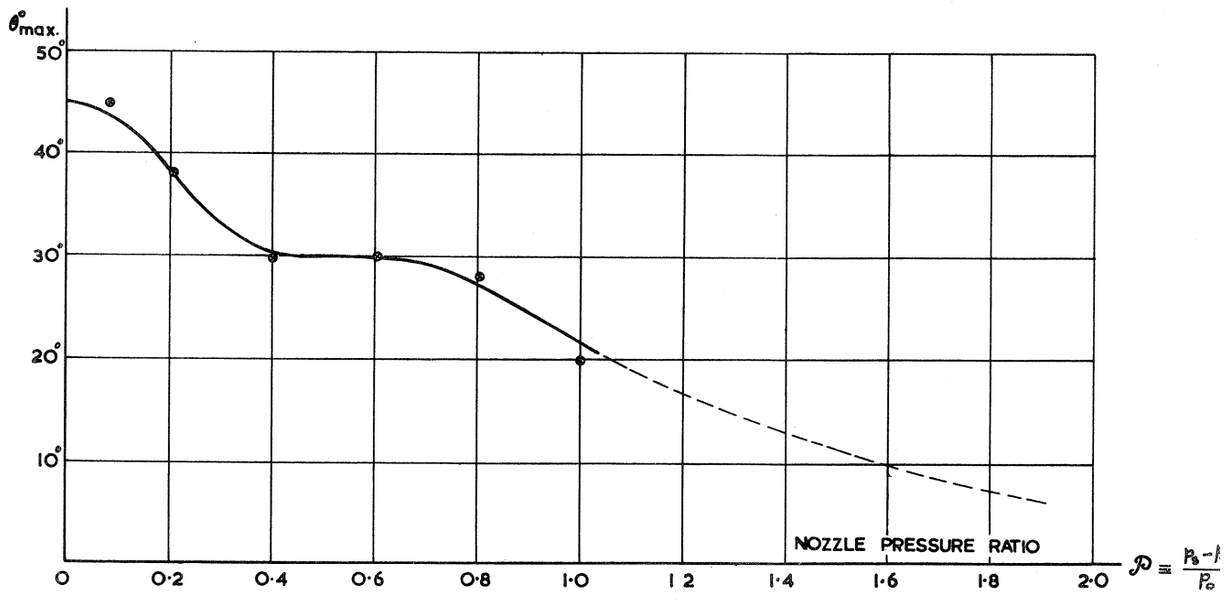

FIG. 18. THE VARIATION OF THE ANGLE FOR MAXIMUM TOTAL NOISE INTENSITY WITH JET SPEED.

$\frac{\tilde{\omega}}{d} = 108.$

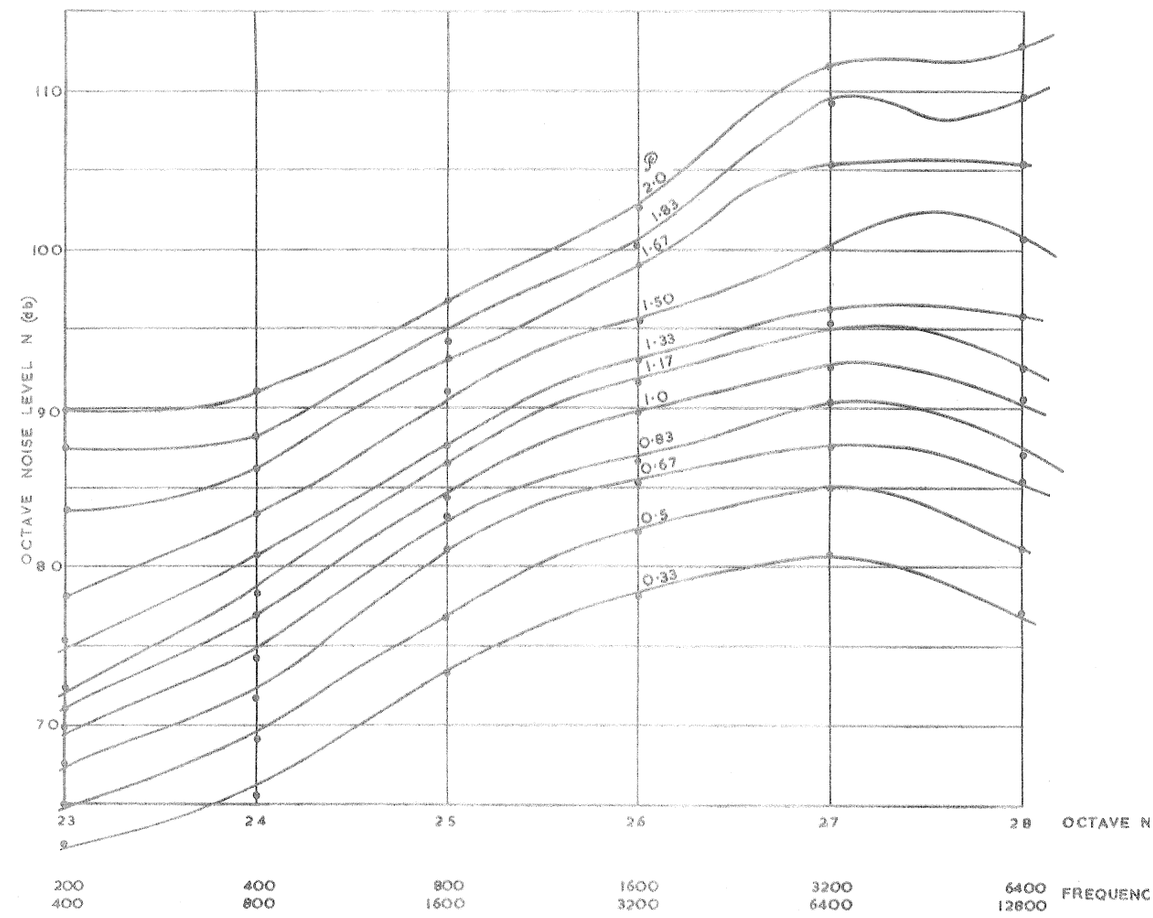

FIG. 19. THE NOISE LEVEL SPECTRUM, (EFFECT OF JET SPEED) (MICROPHONE CORRECTION APPLIED). θ=9

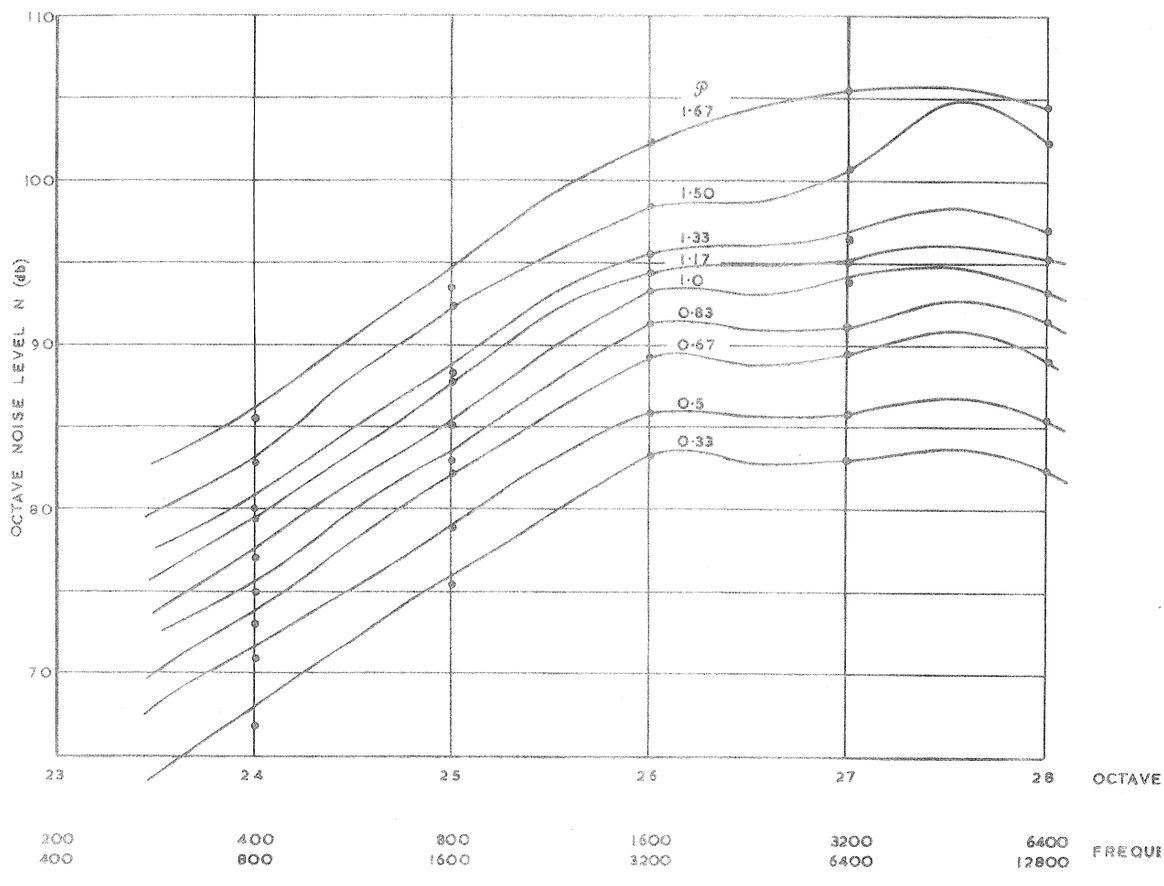

FIG. 20. THE NOISE LEVEL SPECTRUM, (EFFECT OF JET SPEED) (MICROPHONE CORRECTION APPLIED) θ=

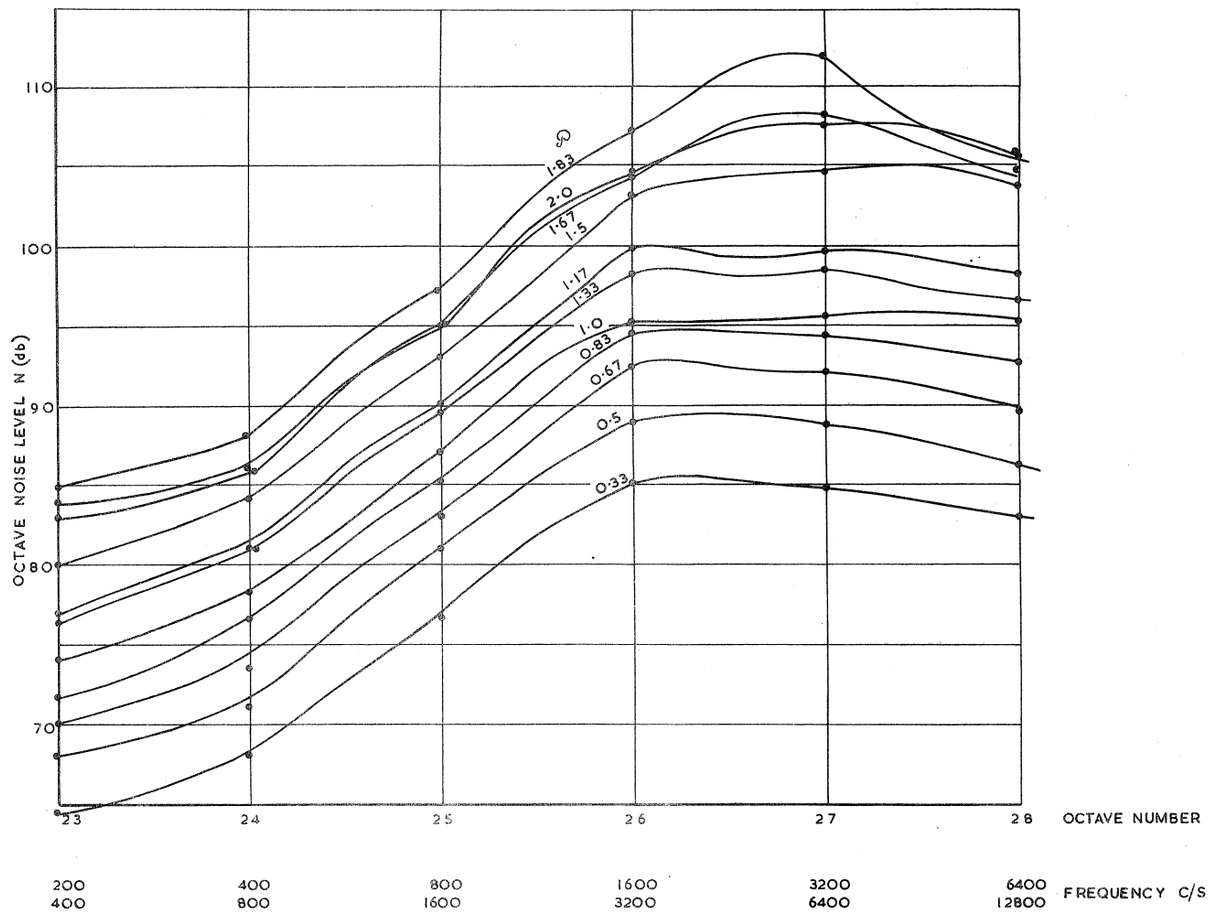

FIG. 21. THE NOISE LEVEL SPECTRUM, (EFFECT OF JET SPEED) (MICROPHONE CORRECTION APPLIED). $\theta = 60^\circ$ $\tilde{\omega}/_d = 108$.

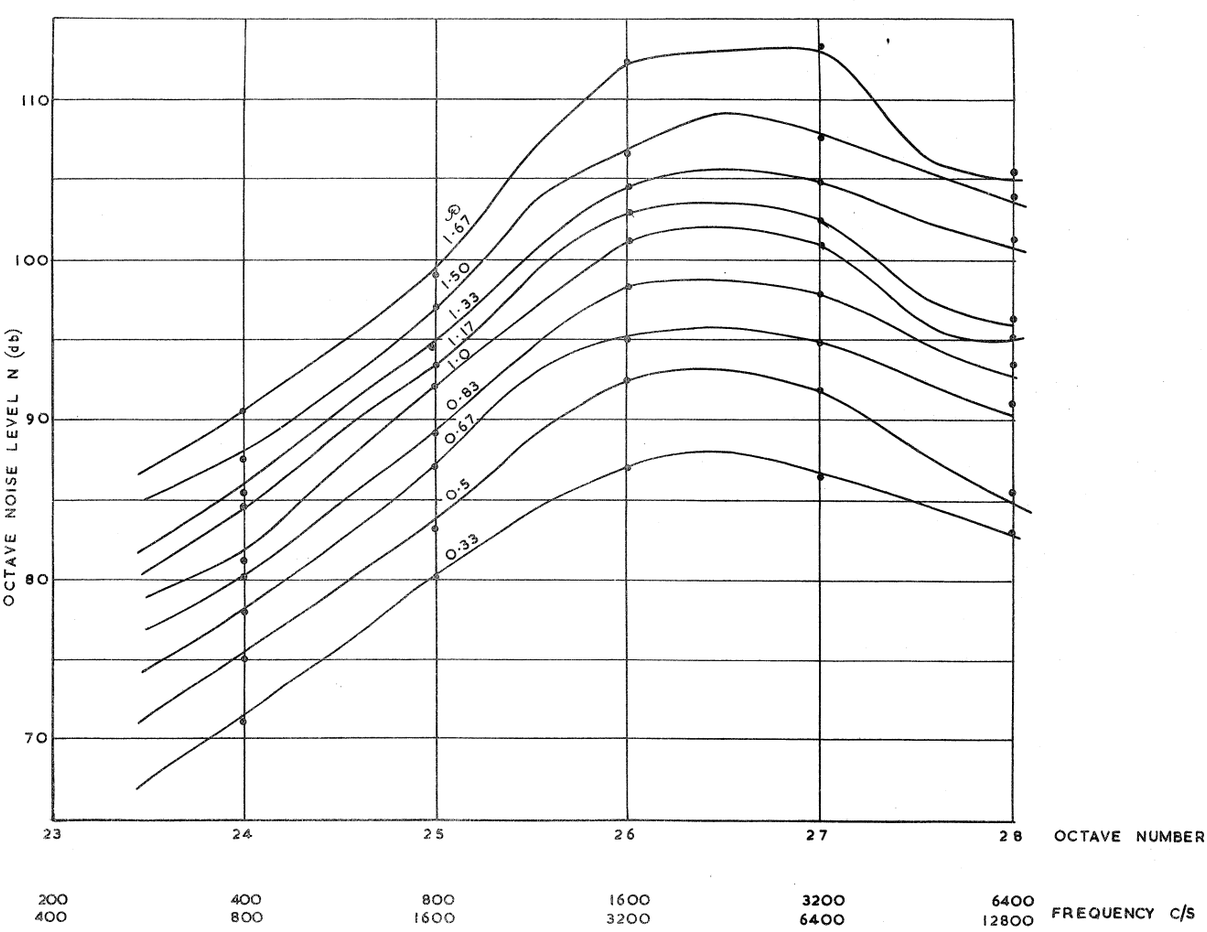

FIG. 22. THE NOISE LEVEL SPECTRUM, (EFFECT OF JET SPEED) (MICROPHONE CORRECTION APPLIED). $\theta = 45^\circ$ $\tilde{\omega}/_d = 108$.

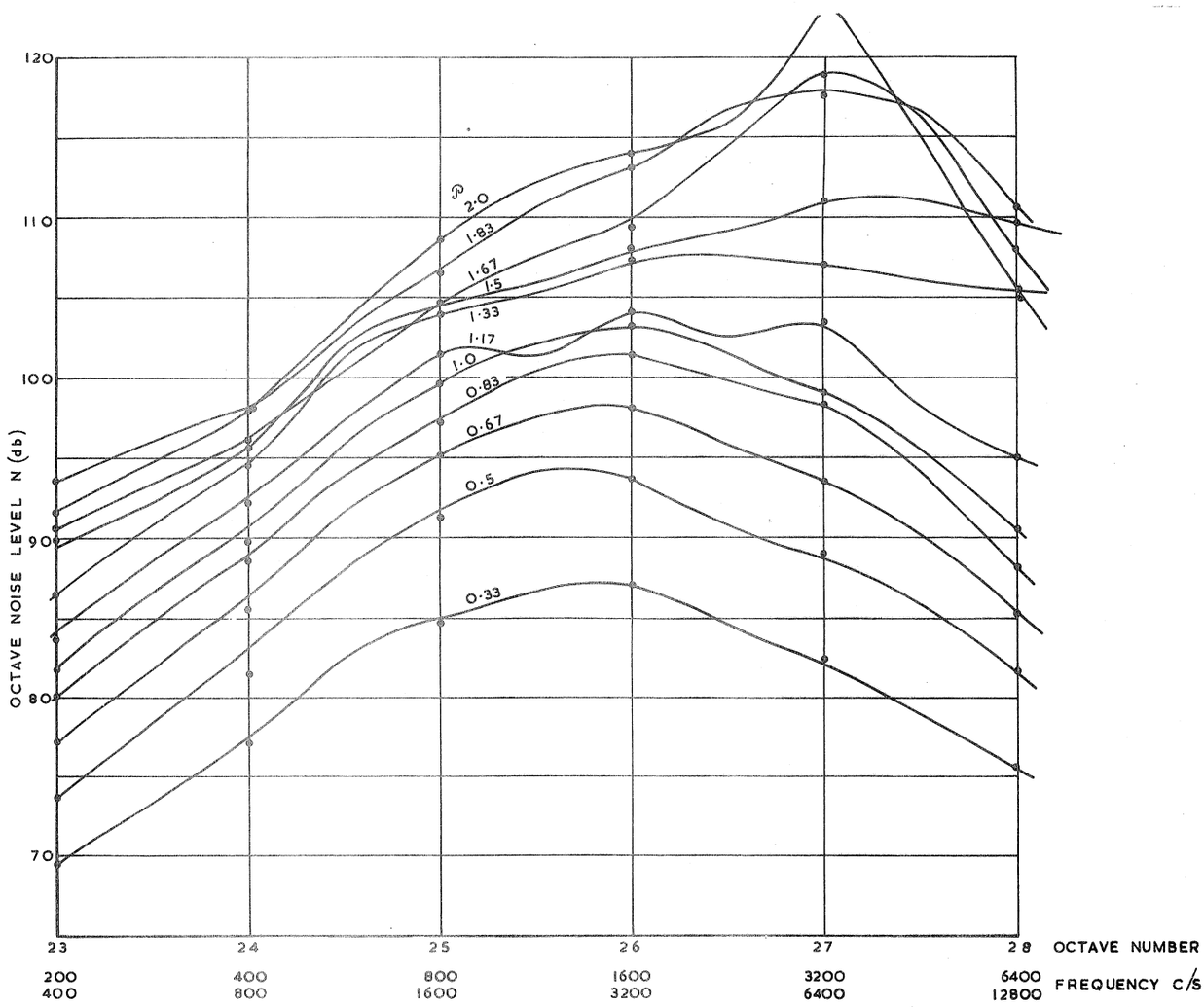

FIG. 23. THE NOISE LEVEL SPECTRUM. (EFFECT OF JET SPEED) (MICROPHONE CORRECTION APPLIED). $\theta = 30^\circ$ $\tilde{\omega}/d = 108$.

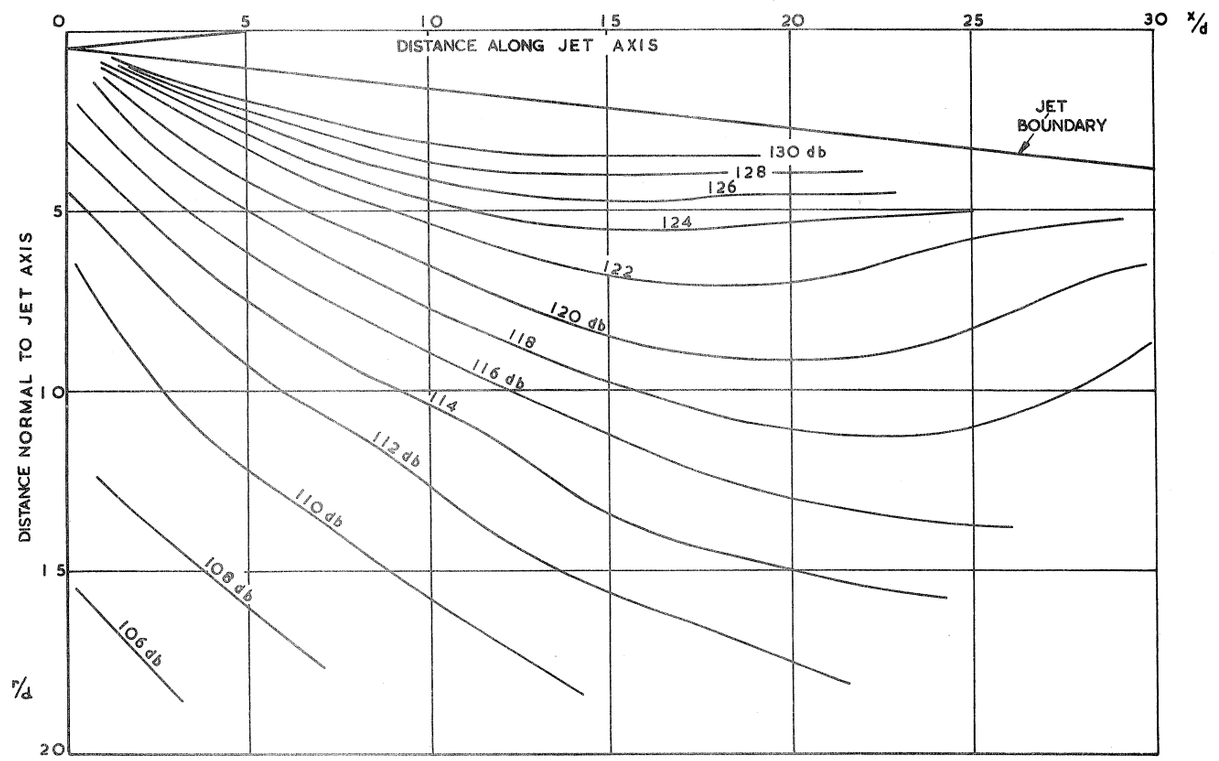

FIG. 24. THE NEAR NOISE FIELD. (MICROPHONE CORRECTION NOT APPLIED). $\mathcal{P}$=0·9 (TOTAL NOISE)

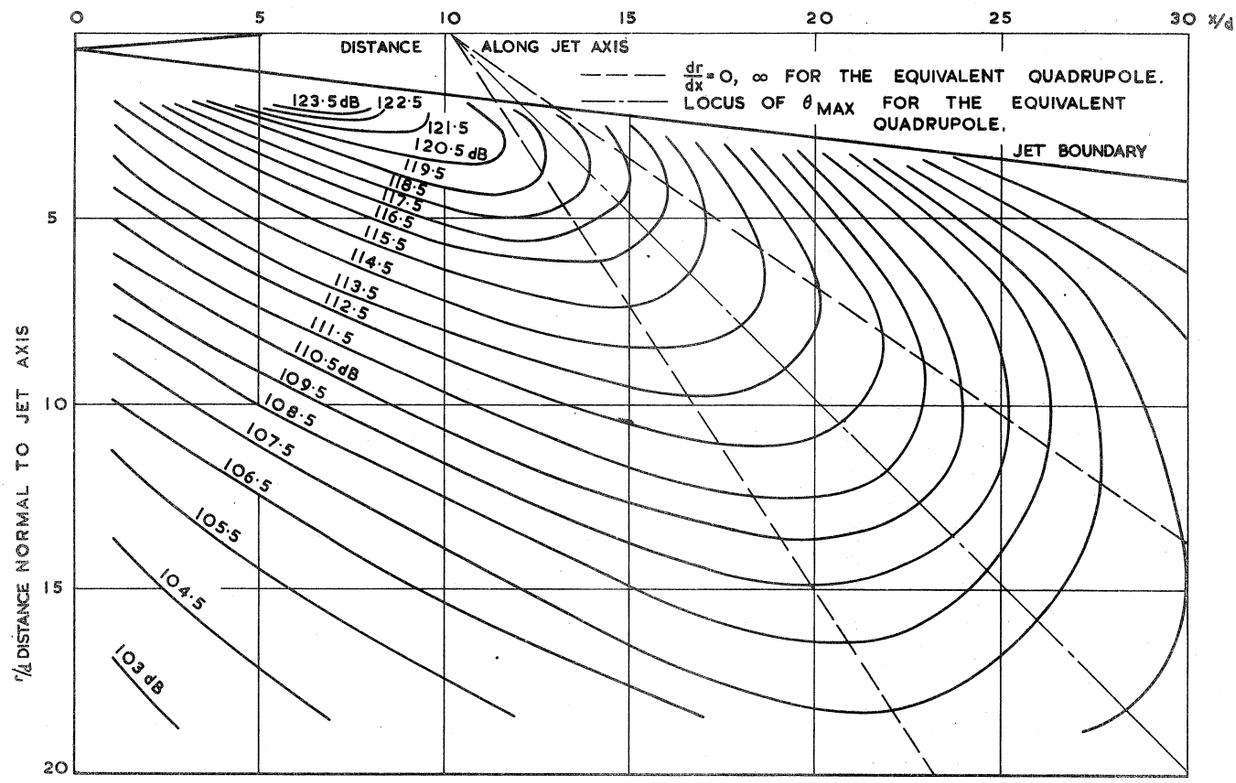

FIG. 25. THE NEAR NOISE FIELD. (MICROPHONE CORRECTION NOT APPLIED.)
OCTAVE NUMBER = 28 $\mathcal{P} = 0{\cdot}9$

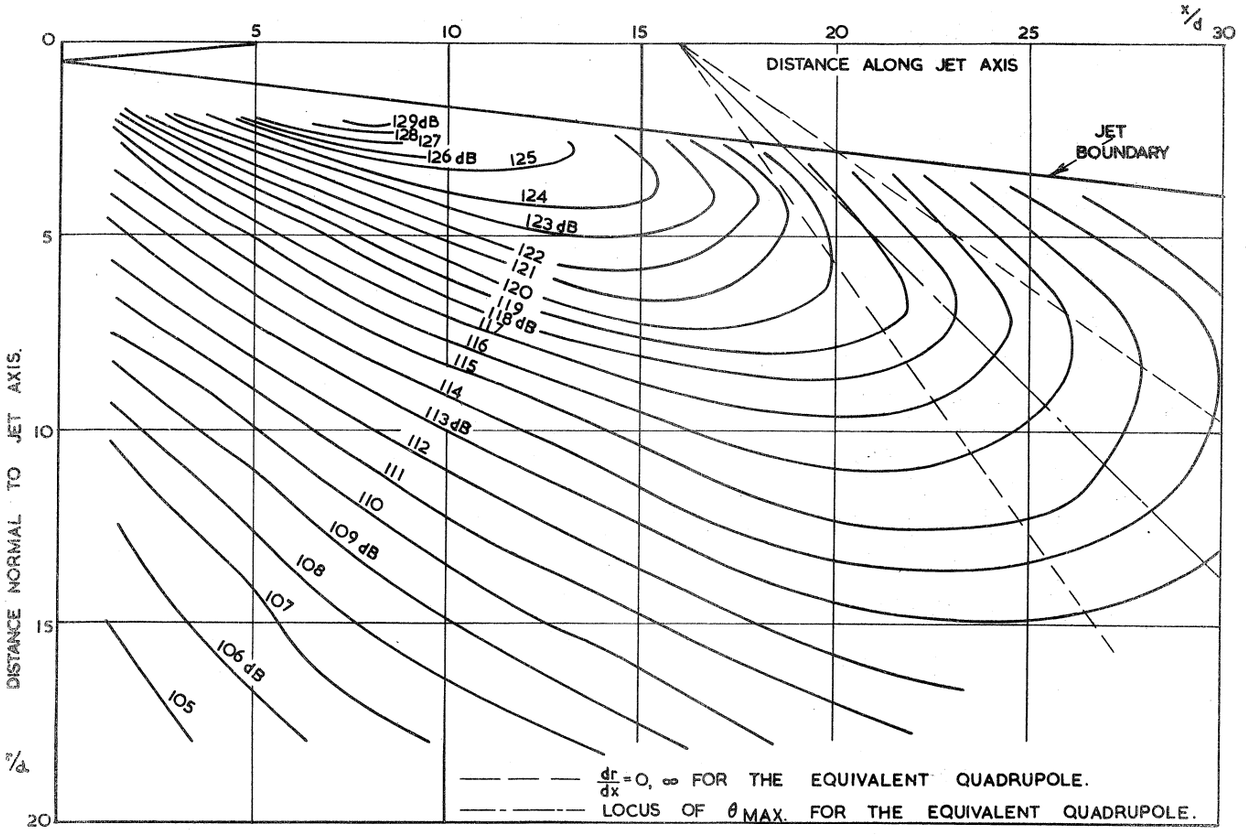

FIG. 26. THE NEAR NOISE FIELD. (MICROPHONE CORRECTION NOT APPLIED.)
OCTAVE NUMBER = 27 $\mathcal{P} = 0{\cdot}9$.

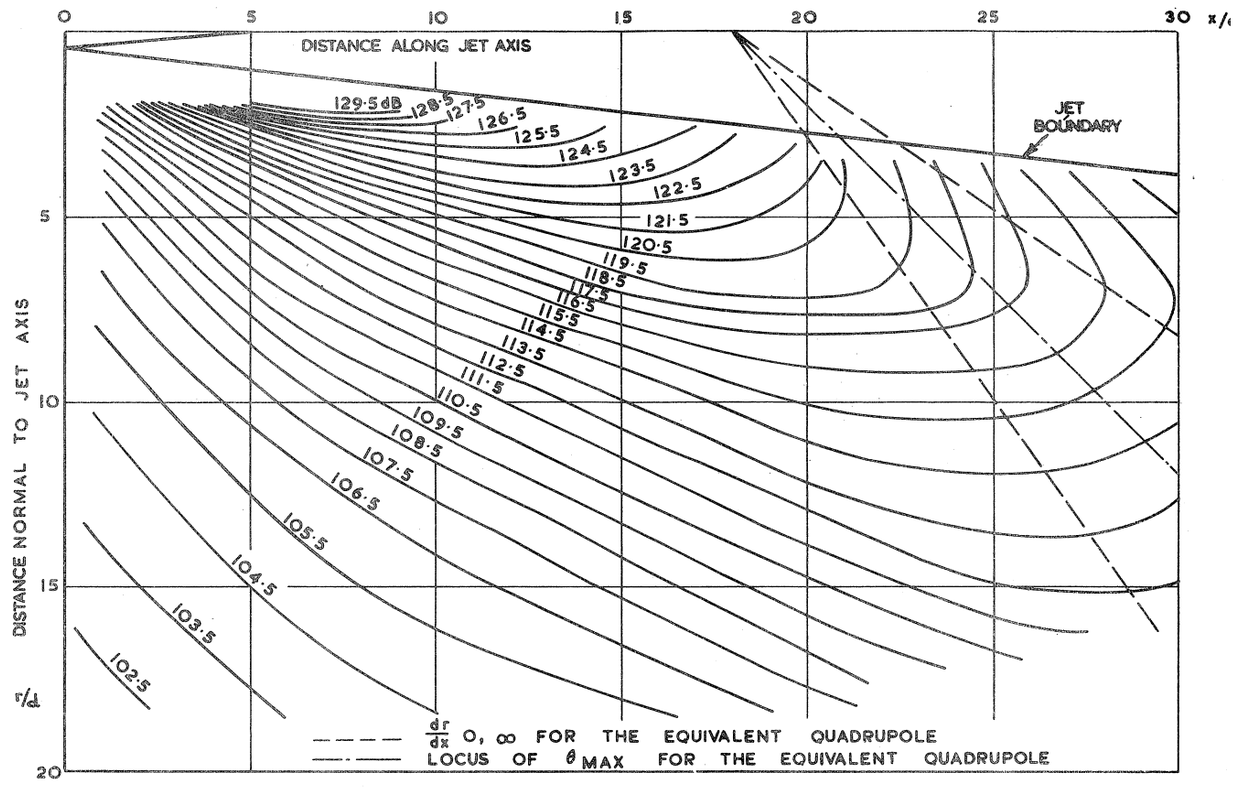

FIG. 27. THE NEAR NOISE FIELD. (MICROPHONE CORRECTION NOT APPLIED.)
OCTAVE NUMBER = 26 $\mathcal{P}$ = 0·9

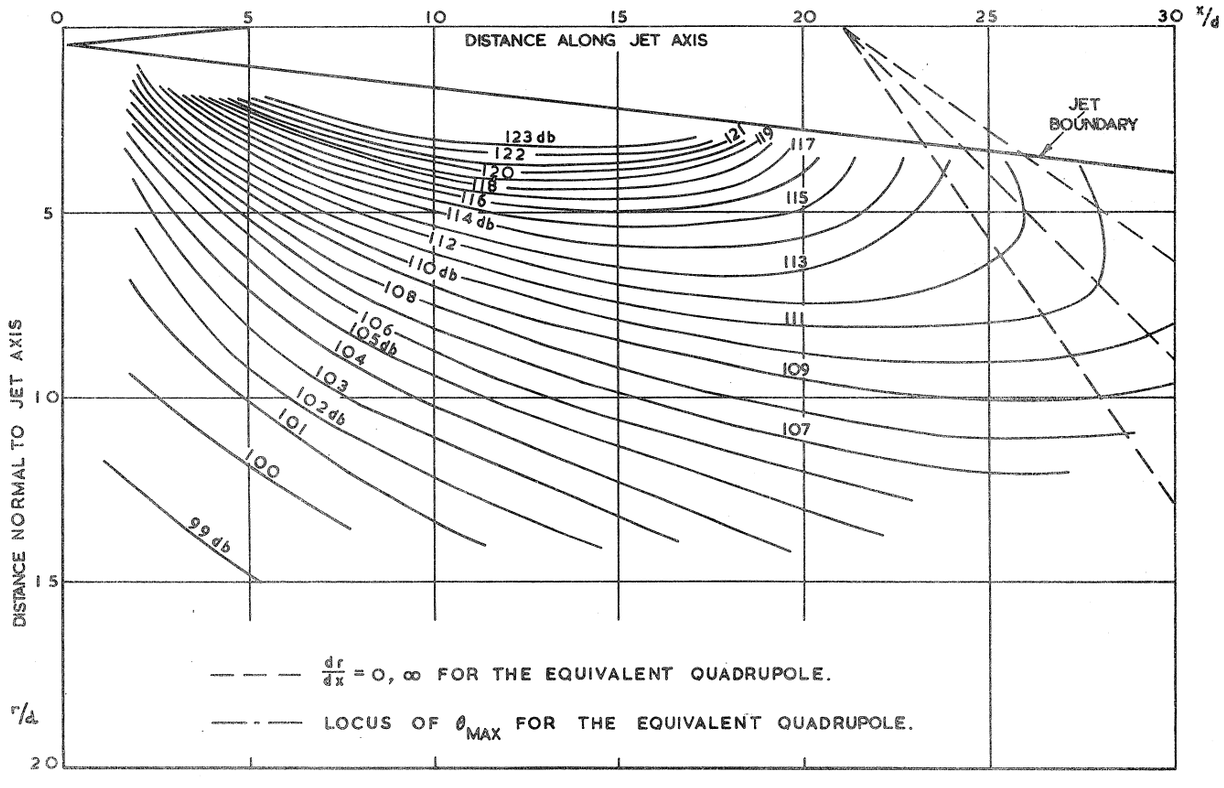

FIG. 28. THE NEAR NOISE FIELD. (MICROPHONE CORRECTION NOT APPLIED).
OCTAVE NUMBER = 25 $\mathcal{P}$ = 0·9

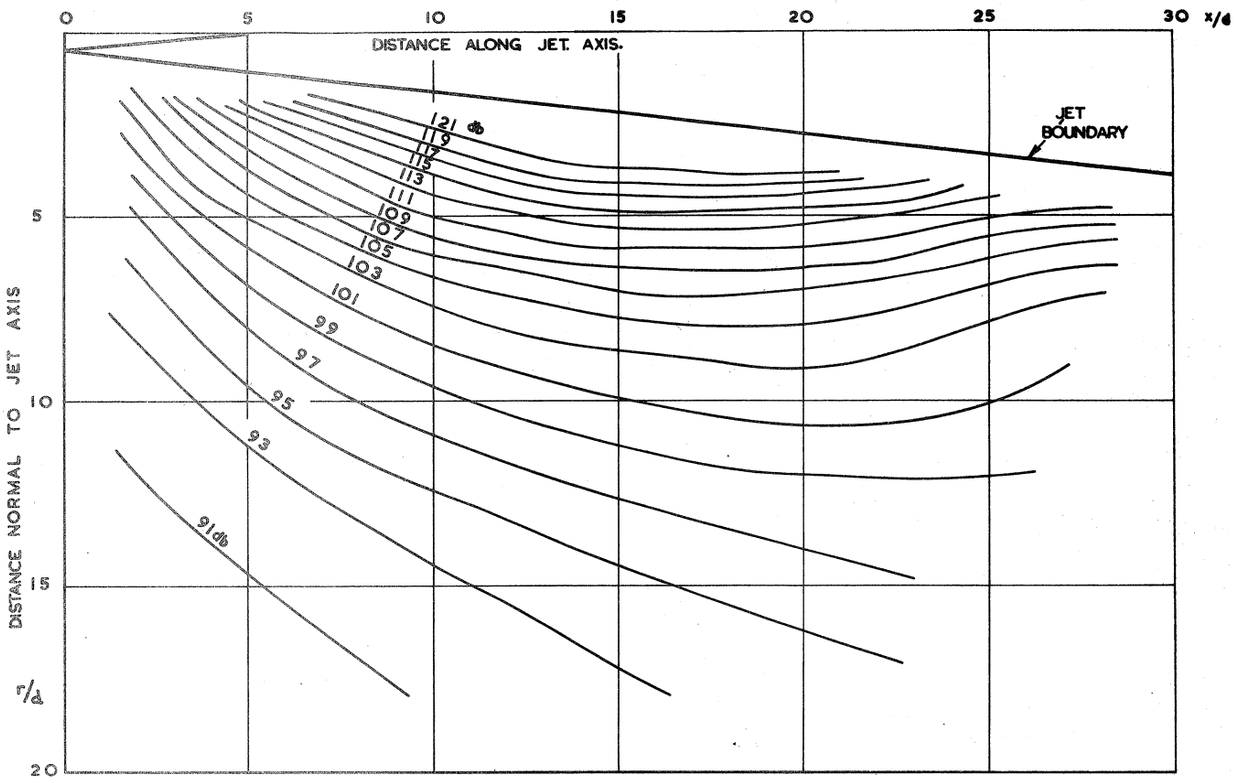

FIG. 29 THE NEAR NOISE FIELD (MICROPHONE CORRECTION NOT APPLIED.)
OCTAVE NUMBER = 24 $\mathcal{P}$ = 0·9

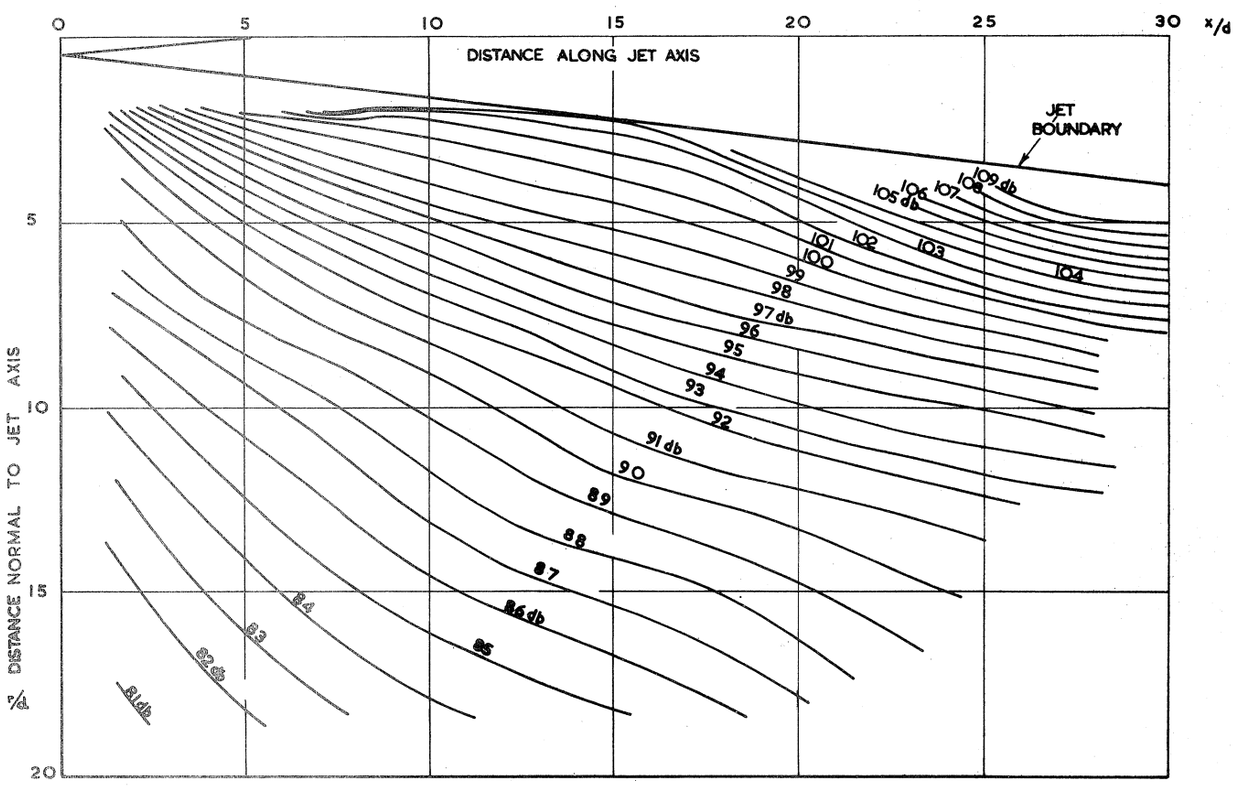

FIG. 30. THE NEAR NOISE FIELD (MICROPHONE CORRECTION NOT APPLIED)
OCTAVE NUMBER 11 $\mathcal{P}$ = 0·9

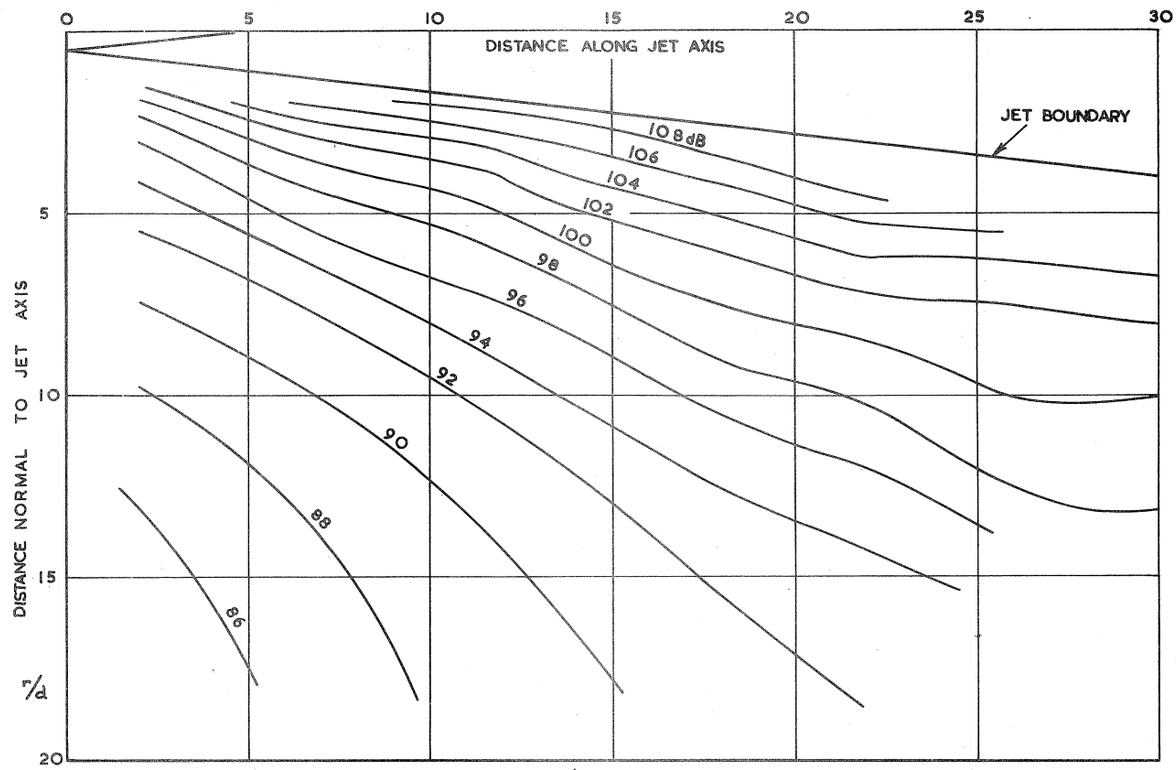

FIG. 33. THE NEAR NOISE FIELD (MICROPHONE CORRECTION NOT APPLIED)
OCTAVE NUMBER = 11 $\mathcal{P}$ = 1·33

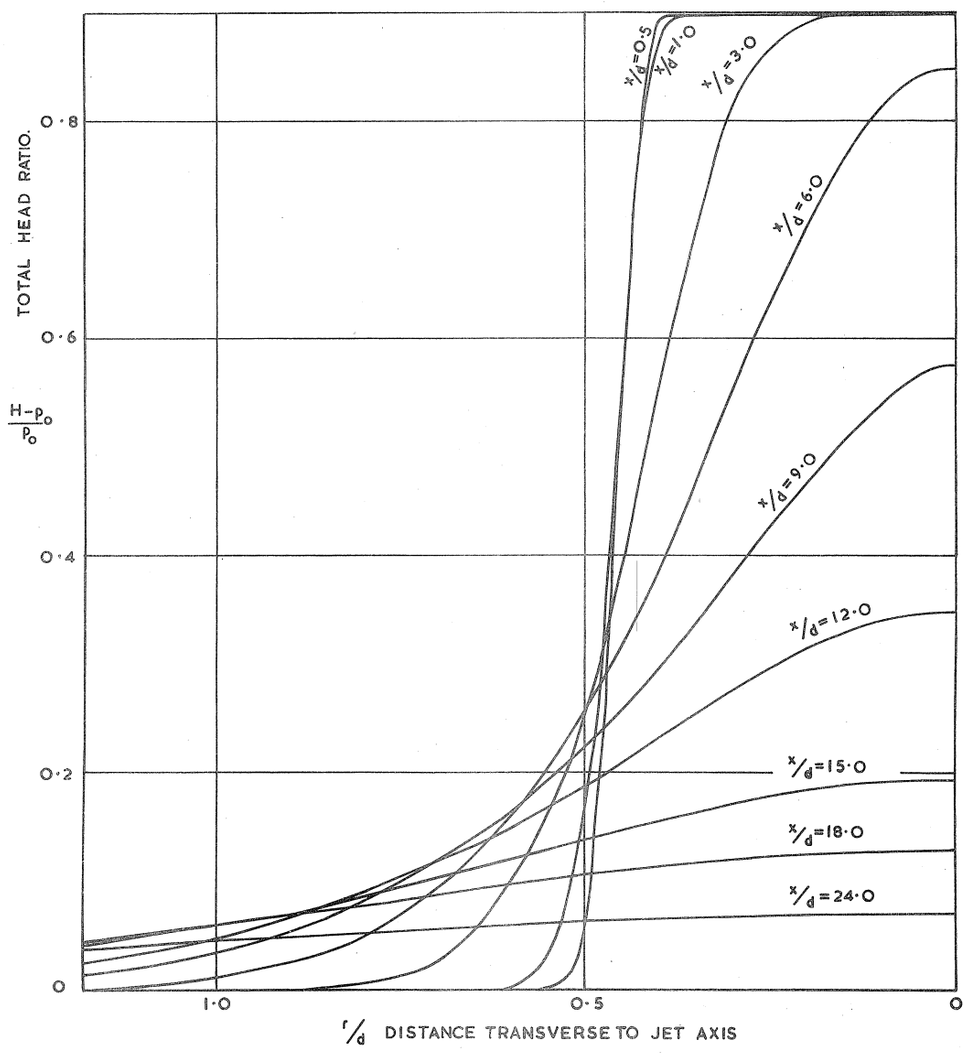

FIG. 34. THE DISTRIBUTIONS OF TOTAL HEAD ACROSS THE JET. $\mathcal{P}$ = 0·9.

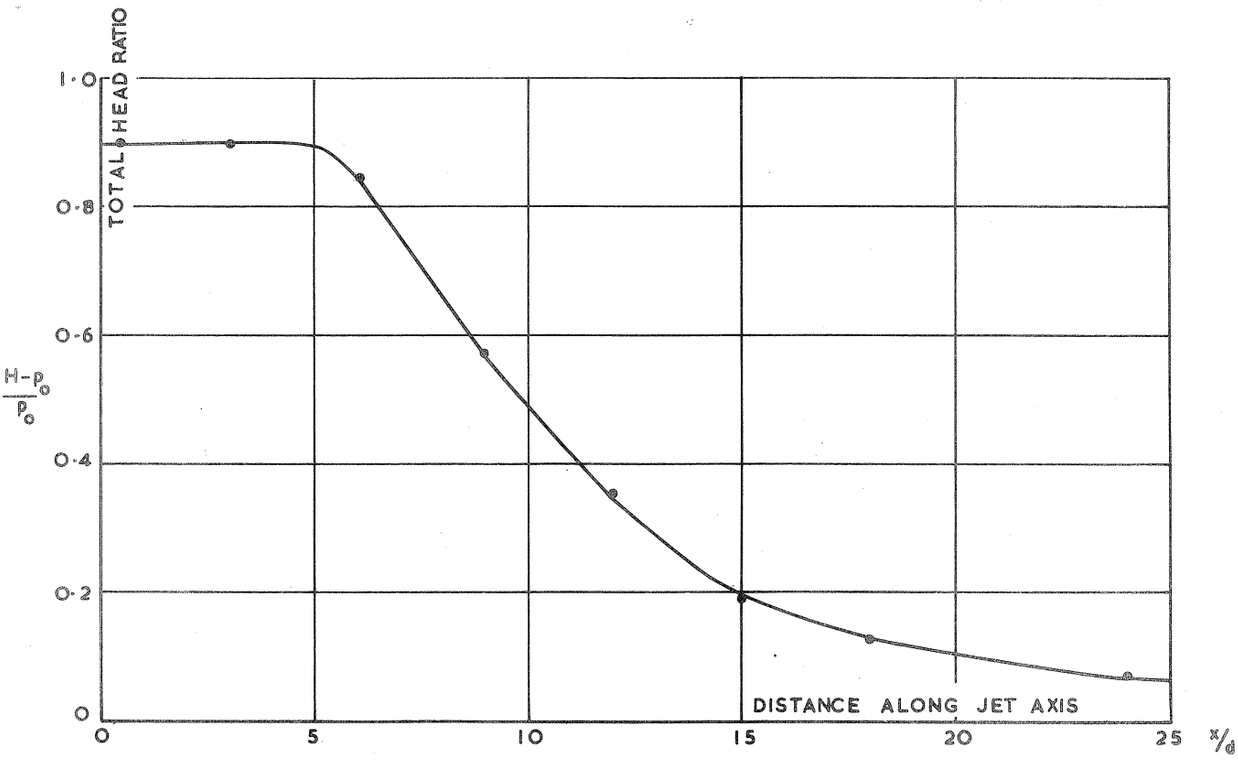

FIG. 35. THE VARIATION OF TOTAL HEAD ALONG THE JET AXIS. $\mathcal{P}$=0·9.

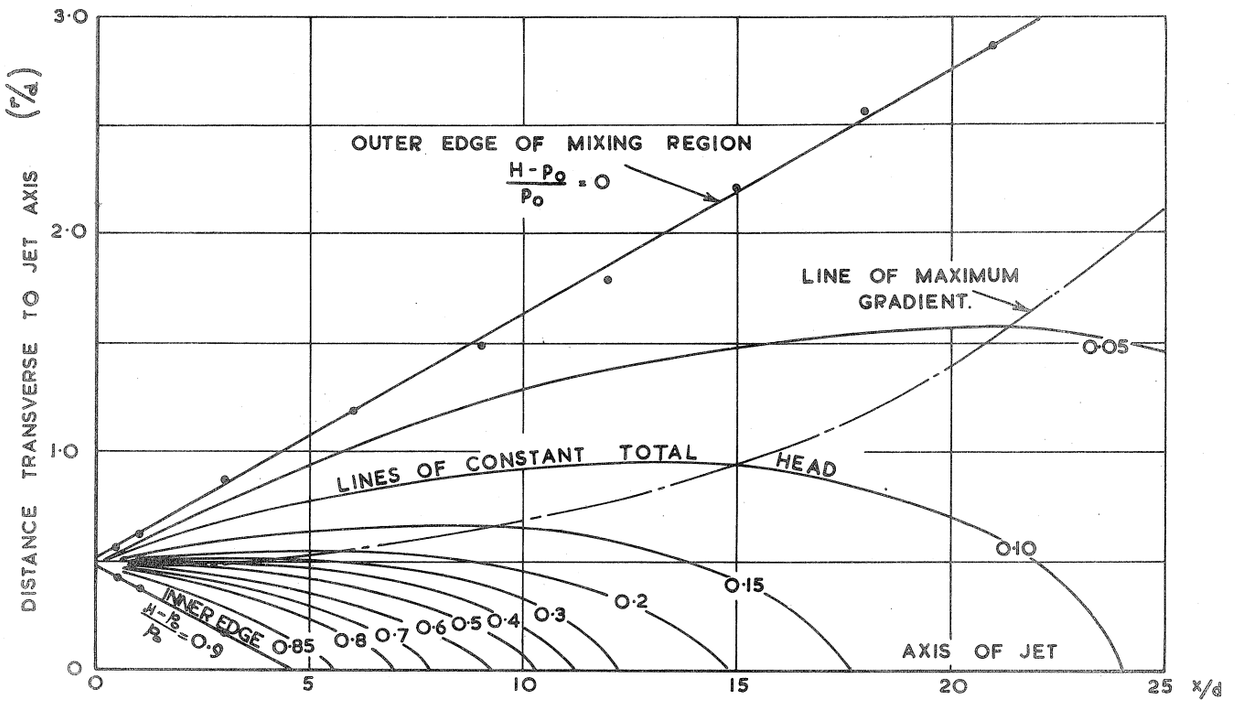

FIG 36. THE BOUNDARIES OF THE JET AND THE MIXING REGION $\mathcal{P}$ = 0·9

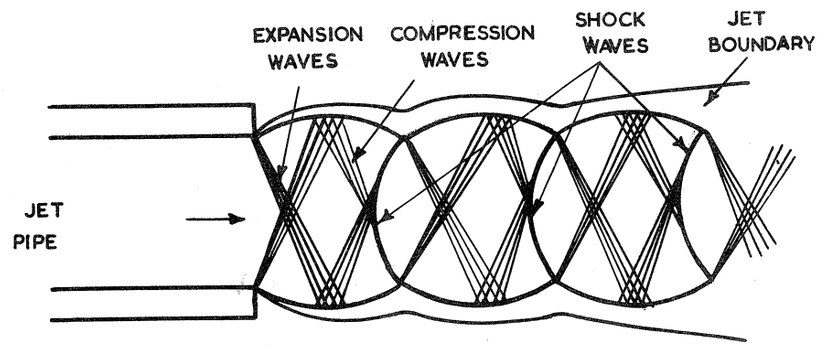

(A)

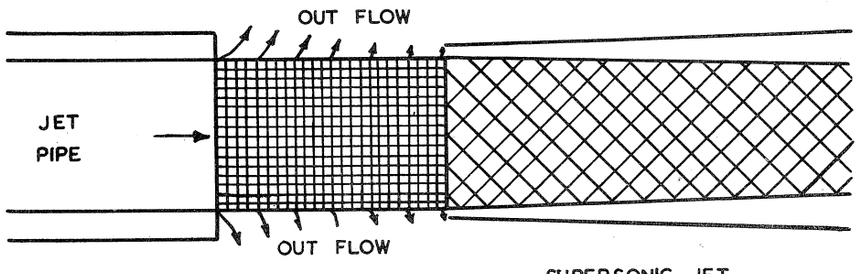

(B)

FIG. 37. THE EFFECT OF ADDING A POROUS EXTENSION TO A JET PIPE WHEN THE STATIC PRESSURE AT THE JET PIPE EXIT EXCEEDS ATMOSPHERIC PRESSURE

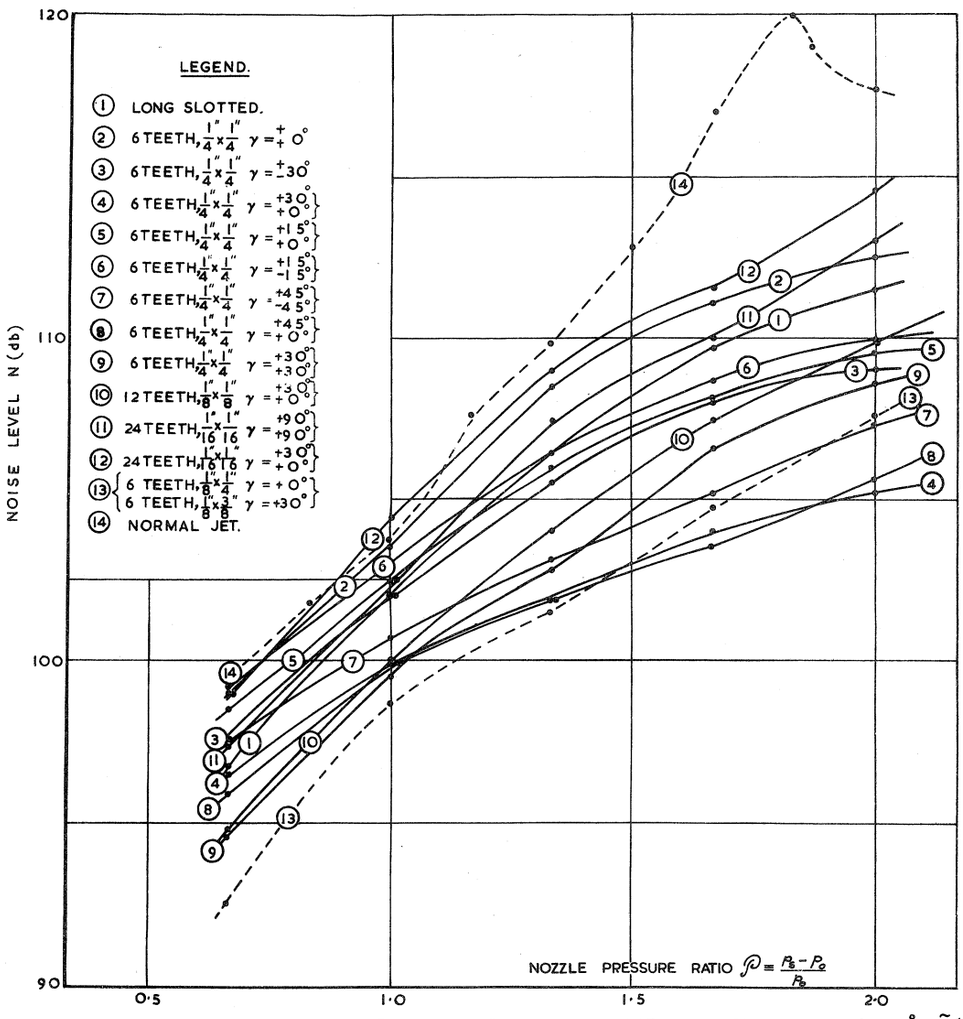

FIG. 38. THE EFFECT OF JET TEETH ON TOTAL NOISE — VARIATION WITH JET SPEED. $\theta = 30°$ $\tilde{\omega}/d = 108$.

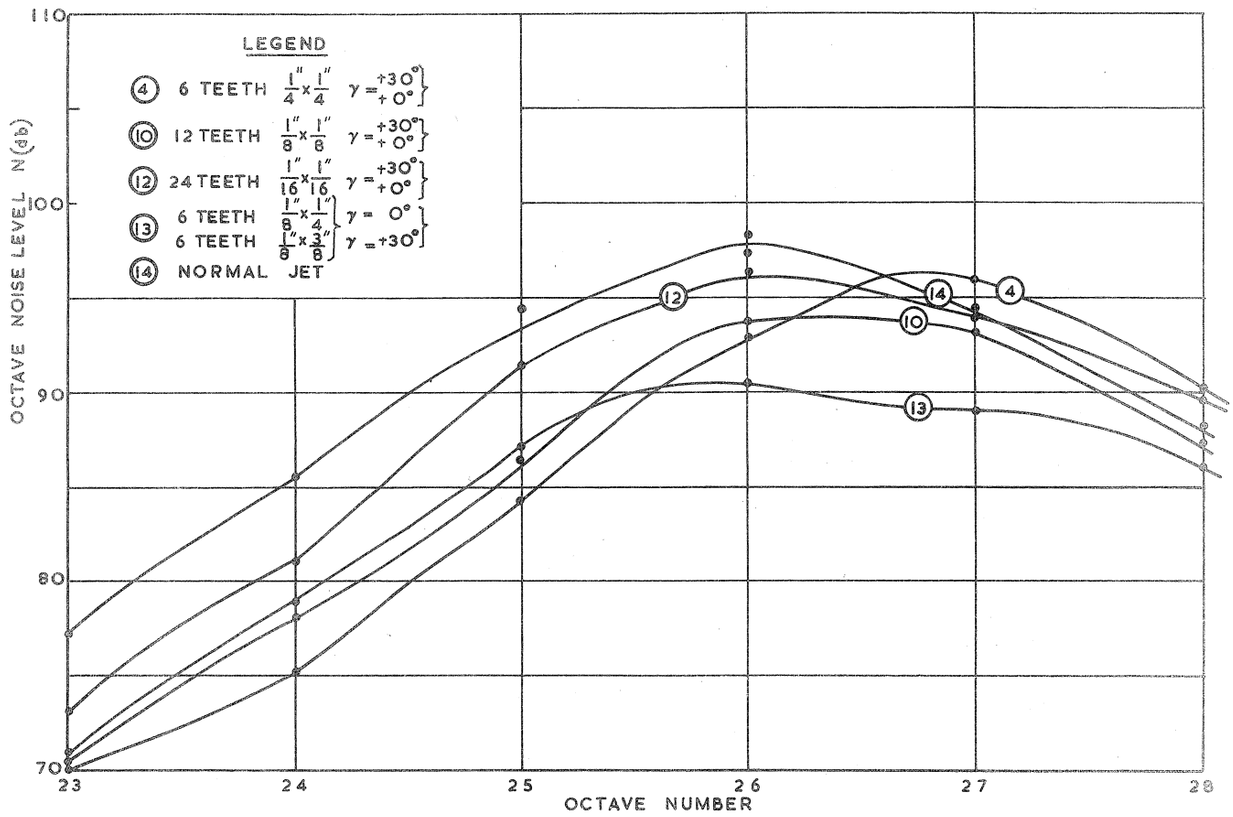

FIG. 39. THE EFFECT OF JET TEETH ON THE NOISE SPECTRUM.

$\mathcal{P}$=0·67 θ=30° $\tilde{\omega}/_{d}$=108

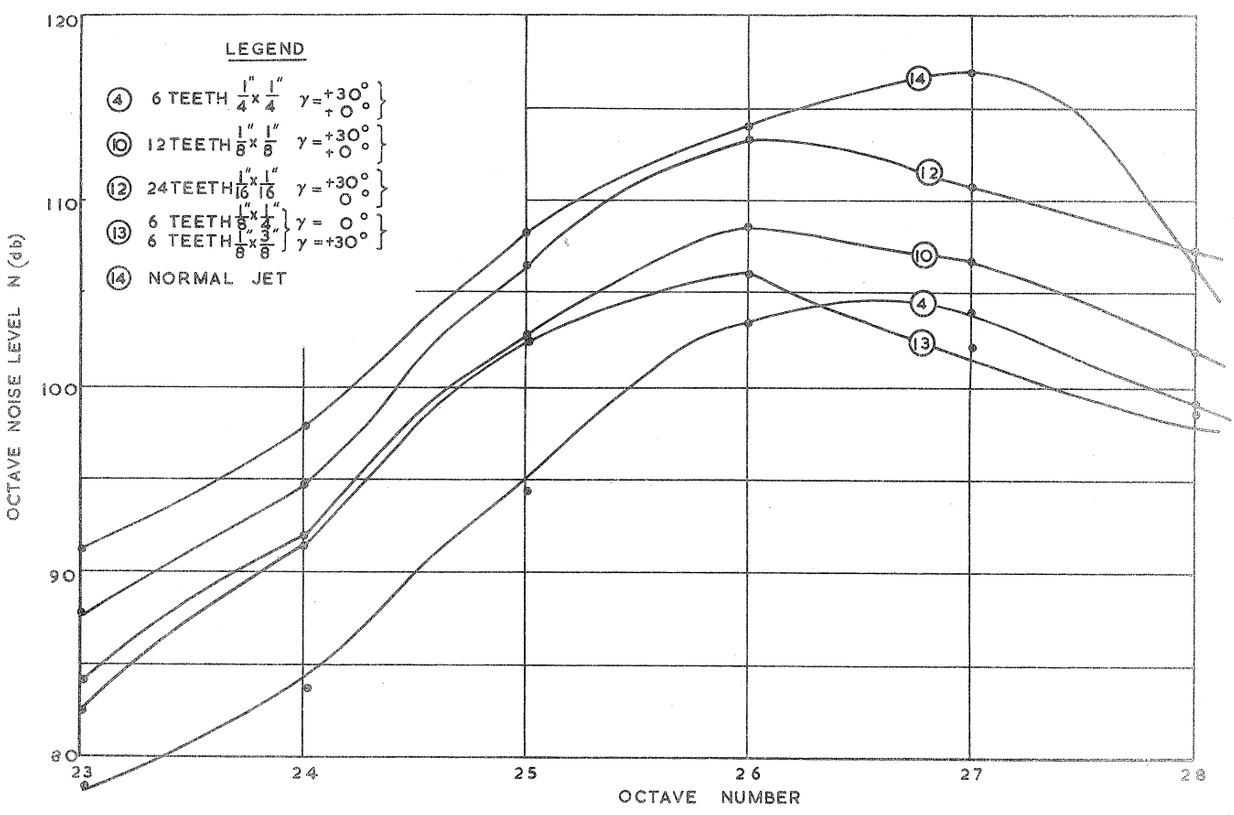

FIG. 40. THE EFFECT OF JET TEETH ON THE NOISE SPECTRUM.

$\mathcal{P}$ = 2·0 θ = 30° $\tilde{\omega}/_{d}$ = 108.

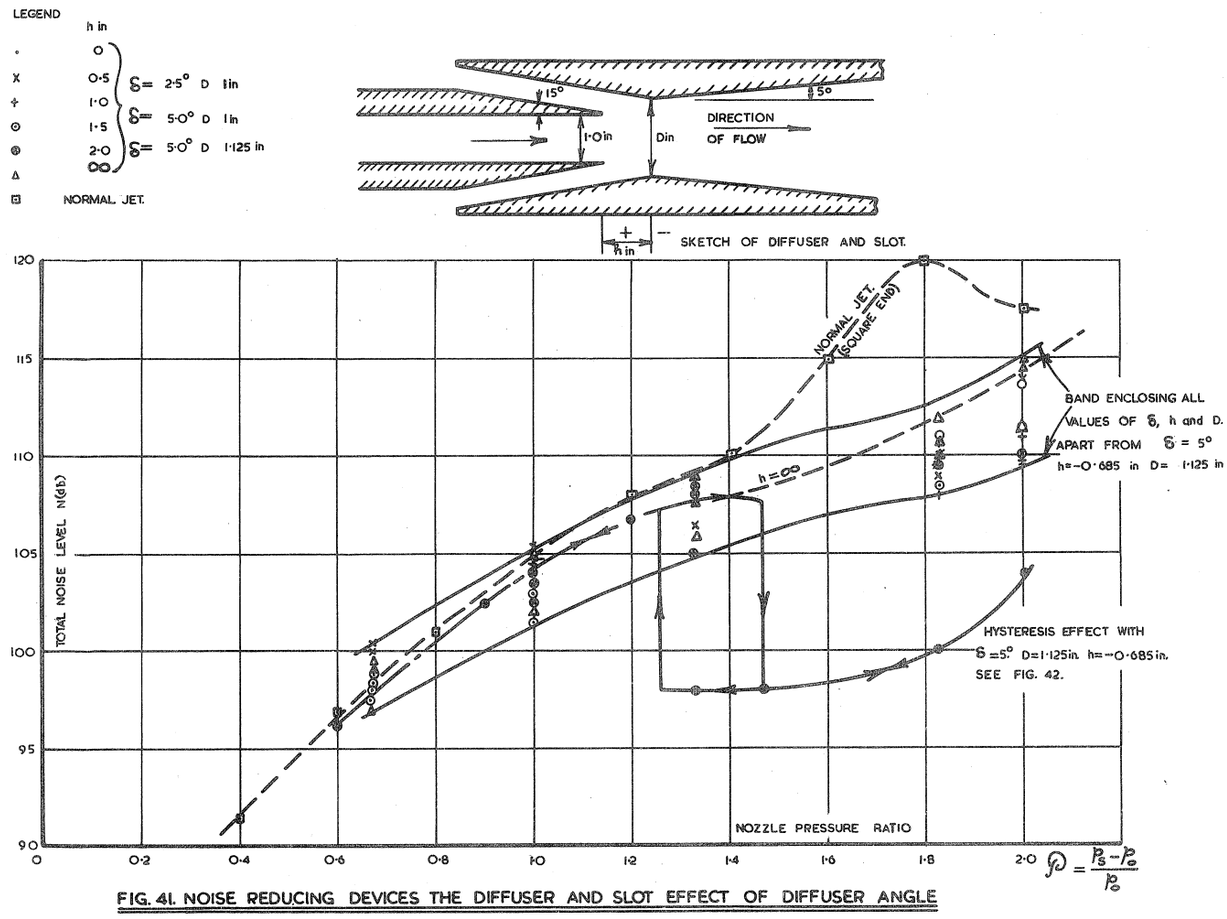

FIG. 41. NOISE REDUCING DEVICES THE DIFFUSER AND SLOT EFFECT OF DIFFUSER ANGLE THROAT DIAMETER AND GAP

$\frac{\tilde{\omega}}{d} = 108 \quad \Theta = 30°$

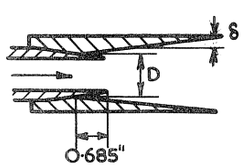

$\frac{\tilde{\omega}}{d} = 108 \quad \Theta = 30°$

DIFFUSER ANGLE (δ) 5°

THROAT DIAMETER (D) 1·125"

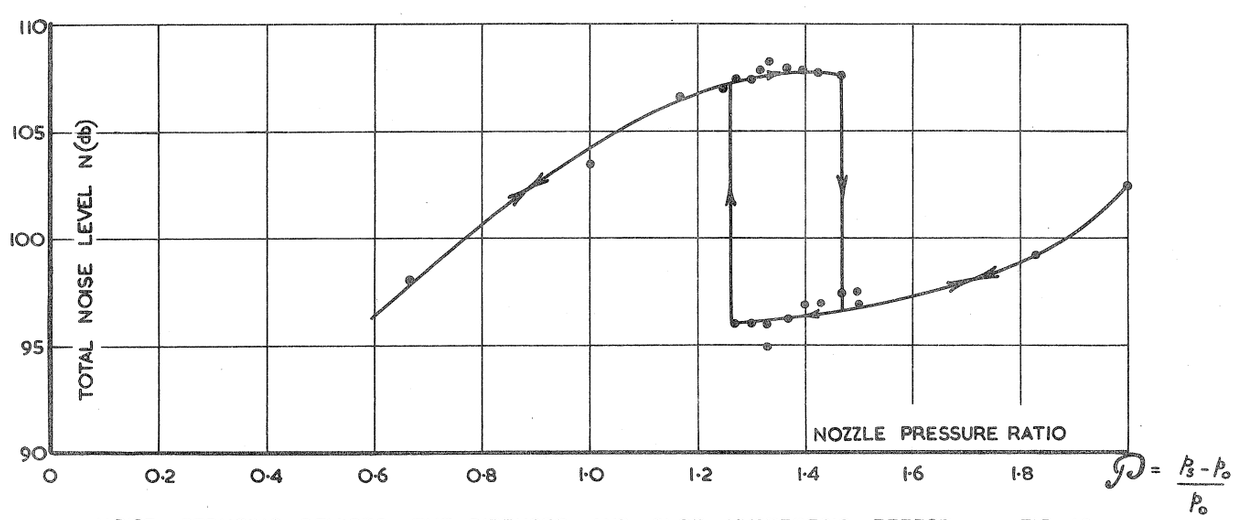

NOISE REDUCING DEVICES. THE DIFFUSER AND SLOT. HYSTERESIS EFFECT. FIG. 42.

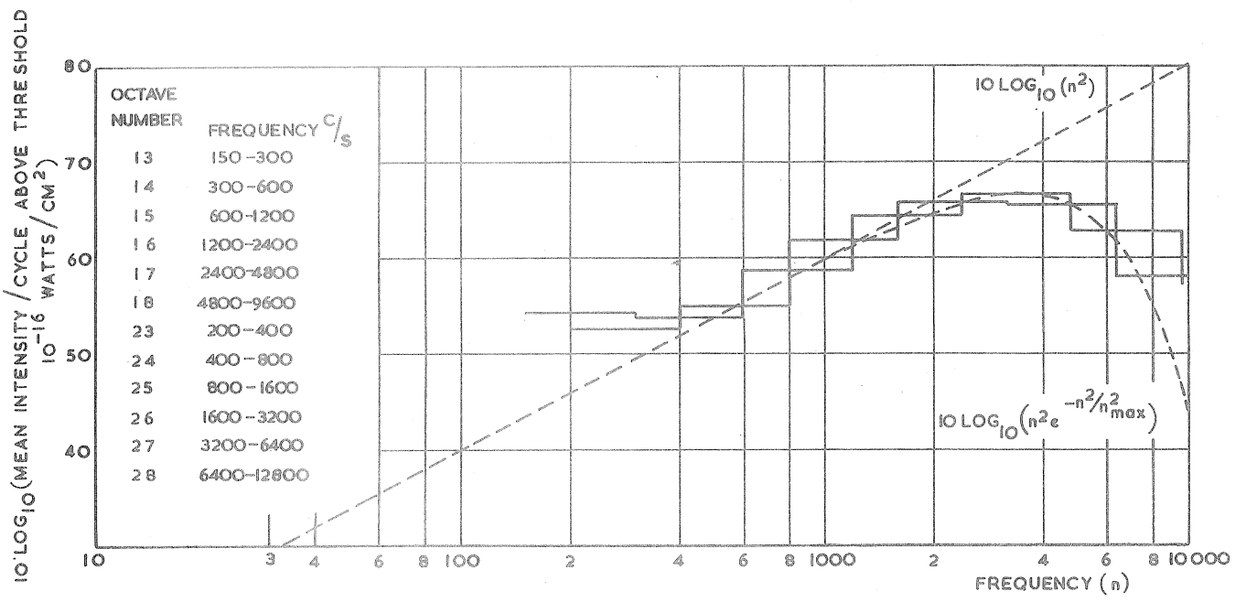

FIG. 43. TYPICAL NOISE SPECTRUM. $\theta = 45^\circ$ $\tilde{\omega}/a = 108$ $P = 0.9$.

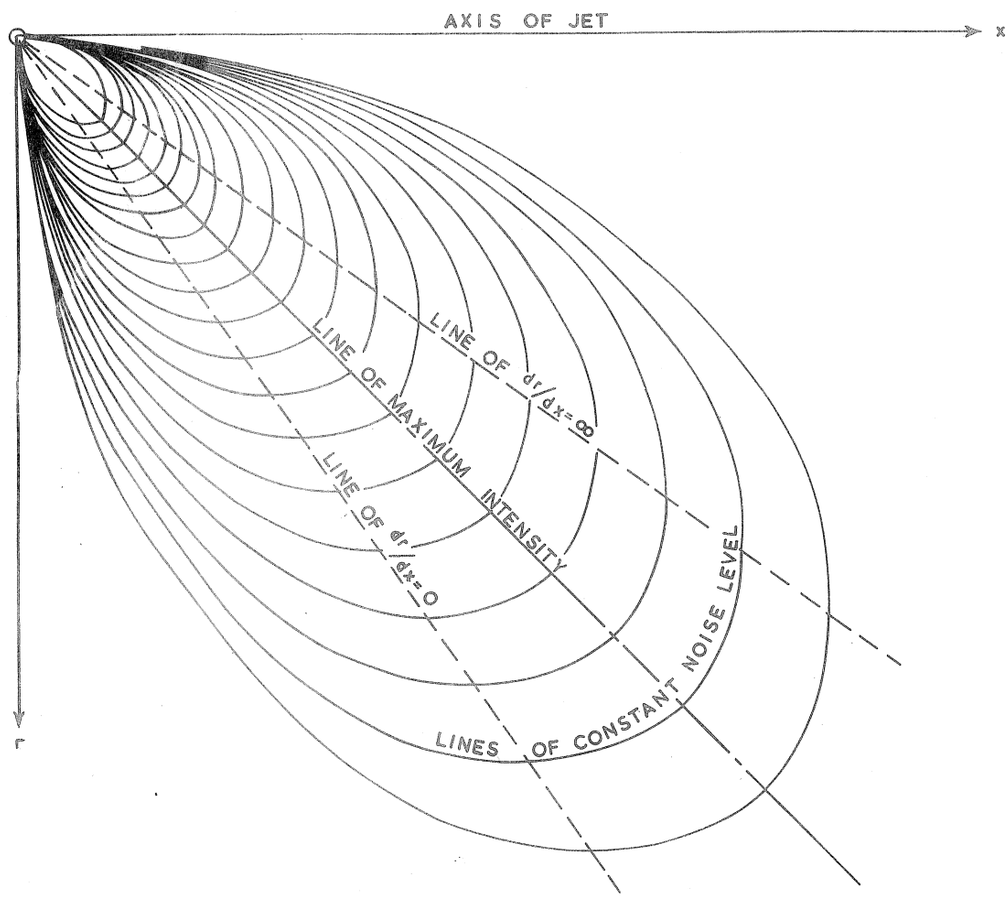

FIG. 44. THE SOUND FIELD DUE TO A POINT QUADRUPOLE AT THE ORIGIN. (ONE QUADRANT ONLY).